Simulating propagation of separated wave modes in general anisotropic media, Part I: qP-wave propagators[a]

[a]Published in Geophysics, 79, no. 1, C1-C18, (2014)

Jiubing Cheng[1] *and Wei Kang*[2]

ABSTRACT

Wave propagation in an anisotropic medium is inherently described by elastic wave equations, with P- and S-wave modes intrinsically coupled. We present an approach to simulate propagation of separated wave modes for forward modeling, migration, waveform inversion and other applications in general anisotropic media. The proposed approach consists of two cascaded computational steps. First, we simulate equivalent elastic anisotropic wavefields with a minimal second-order coupled system (that we call here a pseudo-pure-mode wave equation), which describes propagation of all wave modes with a partial wave mode separation. Such a system for qP-wave is derived from the inverse Fourier transform of the Christoffel equation after a similarity transformation, which aims to project the original vector displacement wavefields onto isotropic references of the polarization directions of qP-waves. It accurately describes the kinematics of all wave modes and enhances qP-waves when the pseudo-pure-mode wavefield components are summed. The second step is a filtering to further project the pseudo-pure-mode wavefields onto the polarization directions of qP-waves so that residual qS-wave energy is removed and scalar qP-wave fields are accurately separated at each time step during wavefield extrapolation. As demonstrated in the numerical examples, pseudo-pure-mode wave equation plus correction of projection deviation provides a robust and flexible tool for simulating propagation of separated wave modes in transversely isotropic and orthorhombic media. The synthetic example of Hess VTI model shows that the pseudo-pure-mode qP-wave equation can be used in prestack reverse-time migration (RTM) applications.

INTRODUCTION

All anisotropy arises from ordered heterogeneity much smaller than the wavelength (Winterstein, 1990). With the increased resolution of seismic data and because of wider seismic acquisition aperture (both with respect to offset and azimuth), there is a growing awareness that an isotropic description of the Earth may no longer be adequate. Anisotropy appears to be a near-ubiquitous property of earth materials, and its effects on seismic data must be quantified.

Wave equation is the central ingredient in characterizing wave propagation for seismic imaging and elastic parameters inversion. In isotropic media, it is common to use scalar acoustic wave equations to describe the propagation of seismic data as representing only P-wave energy (Yilmaz, 2001). Compared to the elastic wave equation, the acoustic wave equation is simpler and more efficient to use, and does not yield S-waves for modeling of P-waves. Anisotropic media are inherently described by elastic wave equations with P- and S-wave modes intrinsically coupled. It is well known that a S-wave passing through an anisotropic medium splits into two mutually orthogonal waves (Crampin, 1984). Generally the P-wave and the two S-waves are not polarized parallel and perpendicular to the wave vector, thus are called quasi-P (qP) and qausi-S (qS) waves. However, most anisotropic migration implementations do not use the full elastic anisotropic wave equation because of the high computational cost involved, and the difficulties in separating wavefields into different wave modes. Although an acoustic wave does not exist in anisotropic media, Alkhalifah (2000) introduced a pseudo-acoustic approximate dispersion relation for vertically transverse isotropic (VTI) media by setting the shear velocity along the axis of symmetry to zero, which leads to a fourth-order partial differential equation (PDE) in space-time domain. Following the same procedure, he also presented a pseudo-acoustic wave equation of sixth-order in vertical orthorhombic (ORT) anisotropic media (Alkhalifah, 2003). Many authors have implemented pseudo-acoustic VTI modeling and migration based on various coupled second-order PDE systems derived from Alkhalifah's dispersion relation (Alkhalifah, 2000; Klie and Toro, 2001; Zhou et al., 2006b; Hestholm, 2007). Alternatively, coupled first-order and second-order systems are derived starting from first principles (the equations of motion and Hooke's law) under the pseudo-acoustic approximation for VTI media (Duveneck and Bakker, 2011) and recently for orthorhombic media as well (Fowler and King, 2011; Zhang and Zhang, 2011). The pseudo-acoustic tilted transversely isotropic (TTI) or tilted orthorhombic wave equations can be obtained from their pseudo-acoustic VTI (or pseudo-acoustic vertical orthorhombic) counterparts by simply performing a coordinate rotation according to the directions of the symmetry axes (Zhou et al., 2006a; Fletcher et al., 2009). Pseudo-acoustic wave equations have been widely used for RTM in transversely isotropic (TI) media because they describe the kinematic signatures of qP-waves with sufficient accuracy and are simpler than their elastic counterparts, which leads to computational savings in practice.

On the other hand, the pseudo-acoustic approximation may result in some problems in characterizing wave propagation in anisotropic media. First, to enhance computational stability, pseudo-acoustic approximations reduce the freedom to choose the material parameters compared with their elastic counterparts (Grechka et al., 2004). Practitioners often observe instability in practice when the pseudo-acoustic equations are used in complex TI media (Fletcher et al., 2009; Zhang et al., 2011; Bube et al., 2012). Stable RTM implementations in TTI media can be achieved by using pseudo-acoustic wave equations derived directly from first principles (Duveneck and Bakker, 2011) using self-adjoint or covariant derivative operators (Macesanu, 2011; Zhang et al., 2011). Second, the widely-used pseudo-acoustic approximation still results in

significant shear wave presence in both modeling data and RTM images (Zhang et al., 2003; Grechka et al., 2004; Jin et al., 2011). It is not easy to get rid of qSV-waves from the wavefields simulated by the pseudo-acoustic wave equations when a full waveform modeling for qP-wave is required. Placing both sources and receivers into an artificial isotropic or elliptic anisotropic acoustic layer could eliminate many of the undesired qSV-wave energy (Alkhalifah, 2000), but the propagated qP-wave may get converted to qSV-wave and the qSV-wave might get converted back to qP-wave in other portions of the model. A projection filtering based on an approximate representation of characteristic-waveform of qP-waves was suggested to suppress undesired qSV-wave energy at each output time step (Zhang et al., 2009). But qS-wave artifacts still remain and qP-wave amplitudes may be not correctly restored due to the approximation introduced in the used wave equation. To avoid the qSV-wave energy completely, different approaches have recently been proposed to model the pure qP-wave propagation in VTI and TTI media. The optimized separable approximation (Liu et al., 2009; Zhang and Zhang, 2009; Du et al., 2010), the pseudo-analytical method (Etgen and Brandsberg-Dahl, 2009), the low-rank approximation (Fomel et al., 2013), the Fourier finite-difference method (Song and Fomel, 2011) and the rapid expansion method (Pestana and Stoffa, 2010) belong to this category.

In fact, anisotropic phenomena are especially noticeable in shear and mode-converted wavefields. Therefore, modeling of anisotropic shear waves may be important both on theoretical and practical aspects. Liu et al. (2009) factorized the pseudo-acoustic VTI dispersion relation and obtained two pseudo-partial differential (PPD) equations, of which the qP-wave equation is well-posed for any value of the anisotropic parameters, but the qSV-wave equation becomes well-posed only when the condition $\epsilon > \delta$ is satisfied. These PPD equations are very hard to solve in heterogeneous media unless further approximations are introduced (Liu et al., 2009; Chu et al., 2011) or recently developed FFT-based approaches are used (Pestana et al., 2011; Song and Fomel, 2011; Fomel et al., 2013). Note that some of the above efforts to model pure-mode wavefields suffer from accuracy loss more or less due to the approximations to the phase velocities or dispersion relations. Furthermore, these pure-mode propagators only consider the phase term in wave propagation, so they are appropriate for seismic migration but not necessarily for accurate seismic modeling, which may require taking account of amplitude effects and other elastic phenomena such as mode conversion.

In kinematics, there are various forms equivalent to the original first- or second-order elastic wave equations. Mathematically, analysis of the dispersion relation as matrix eigenvalue system allows one to generate equivalent coupled linear second-order systems by similarity transformations (Fowler et al., 2010). Accordingly, Kang and Cheng (2011) proposed new coupled second-order systems for both qP- and qS-waves in TI media by applying specified similarity transformations to the Christoffel equation. Their coupled system for qP-waves represents dominantly the energy propagation of scalar qP-waves while that for qSV-waves propagates dominantly the scalar qSV-wave energy. However, each of the two systems still contains relatively weak residual energy of the other mode. Cheng and Kang (2012) and Kang and Cheng (2012) called such coupled systems "pseudo-pure-mode wave equations" and further

proposed an approach to get separated qP- or qS-wave data from the pseudo-pure-mode wavefields in general anisotropic media. In the two articles of this series, we demonstrate how to simulate propagation of separated wave-modes based on a new simplified description of wave propagation in general anisotropic media. We shall focus on qP- and qS-waves in each article separately.

The first paper is structured as follows: First, we revisit the plane-wave analysis of the full elastic anisotropic wave equation. Then we introduce a similarity transformation to the Christoffel equation required to derive the pseudo-pure-mode qP-wave equation, and give the simplified forms under pseudo-acoustic or/and isotropic approximations to illustrate the physical interpretation. After that, we discuss how to obtain separated qP-wave data from the extrapolated wavefields coupled with residual qS-waves. Finally, we show numerical examples to demonstrate the features and advantages of our approach in wavefield modeling and RTM in TI and orthorhombic media.

PSEUDO-PURE-MODE COUPLED SYSTEM FOR QP-WAVES

Plane-wave analysis of the elastic wave equation

Vector and component notations are used alternatively throughout the paper. The wave equation in general heterogeneous anisotropic media can be expressed as (Carcione, 2001),

$$\rho\frac{\partial^2\mathbf{u}}{\partial t^2} = [\bigtriangledown\mathbf{C}\bigtriangledown^T]\mathbf{u} + \mathbf{f}, \tag{1}$$

where $\mathbf{u} = (u_x, u_y, u_z)^T$ is the particle displacement vector, $\mathbf{f} = (f_x, f_y, f_z)^T$ represents the force term, ρ is the density, $\mathbf{C}$ is the matrix representing the stiffness tensor in a two-index notation called the Voigt recipe, and the symmetric gradient operator has the following matrix representation:

$$\bigtriangledown = \begin{pmatrix} \frac{\partial}{\partial x} & 0 & 0 & 0 & \frac{\partial}{\partial z} & \frac{\partial}{\partial y} \\ 0 & \frac{\partial}{\partial y} & 0 & \frac{\partial}{\partial z} & 0 & \frac{\partial}{\partial x} \\ 0 & 0 & \frac{\partial}{\partial z} & \frac{\partial}{\partial y} & \frac{\partial}{\partial x} & 0 \end{pmatrix}. \tag{2}$$

Assuming that the material properties vary sufficiently slowly so that spatial derivatives of the stiffnesses can be ignored, equation 1 can be simplified as

$$\rho\frac{\partial^2\mathbf{u}}{\partial t^2} = \Gamma\mathbf{u} + \mathbf{f}, \tag{3}$$

where Γ is the 3×3 symmetric Christoffel differential-operator matrix, of which the elements are given for locally smooth media as follows (Auld, 1973),

$$
\begin{aligned}
\Gamma_{11} &= C_{11}\frac{\partial^2}{\partial x^2} + C_{66}\frac{\partial^2}{\partial y^2} + C_{55}\frac{\partial^2}{\partial z^2} + 2C_{56}\frac{\partial^2}{\partial y \partial z} + 2C_{15}\frac{\partial^2}{\partial x \partial z} + 2C_{16}\frac{\partial^2}{\partial x \partial y}, \\
\Gamma_{22} &= C_{66}\frac{\partial^2}{\partial x^2} + C_{22}\frac{\partial^2}{\partial y^2} + C_{44}\frac{\partial^2}{\partial z^2} + 2C_{24}\frac{\partial^2}{\partial y \partial z} + 2C_{46}\frac{\partial^2}{\partial x \partial z} + 2C_{26}\frac{\partial^2}{\partial x \partial y}, \\
\Gamma_{33} &= C_{55}\frac{\partial^2}{\partial x^2} + C_{44}\frac{\partial^2}{\partial y^2} + C_{33}\frac{\partial^2}{\partial z^2} + 2C_{34}\frac{\partial^2}{\partial y \partial z} + 2C_{35}\frac{\partial^2}{\partial x \partial z} + 2C_{45}\frac{\partial^2}{\partial x \partial y}, \\
\Gamma_{23} &= C_{56}\frac{\partial^2}{\partial x^2} + C_{24}\frac{\partial^2}{\partial y^2} + C_{34}\frac{\partial^2}{\partial z^2} + (C_{44} + C_{23})\frac{\partial^2}{\partial y \partial z} + (C_{36} + C_{45})\frac{\partial^2}{\partial x \partial z} \\
&\quad + (C_{25} + C_{46})\frac{\partial^2}{\partial x \partial y}, \\
\Gamma_{13} &= C_{15}\frac{\partial^2}{\partial x^2} + C_{46}\frac{\partial^2}{\partial y^2} + C_{35}\frac{\partial^2}{\partial z^2} + (C_{45} + C_{36})\frac{\partial^2}{\partial y \partial z} + (C_{13} + C_{55})\frac{\partial^2}{\partial x \partial z} \\
&\quad + (C_{14} + C_{56})\frac{\partial^2}{\partial x \partial y}, \\
\Gamma_{12} &= C_{16}\frac{\partial^2}{\partial x^2} + C_{26}\frac{\partial^2}{\partial y^2} + C_{45}\frac{\partial^2}{\partial z^2} + (C_{46} + C_{25})\frac{\partial^2}{\partial y \partial z} + (C_{14} + C_{56})\frac{\partial^2}{\partial x \partial z} \\
&\quad + (C_{12} + C_{66})\frac{\partial^2}{\partial x \partial y}.
\end{aligned}
\tag{4}
$$

For the most important types of seismic anisotropy such as transverse isotropy and orthorhombic anisotropy, some terms in equation 4 vanish because the corresponding stiffness coefficients become zeros.

Neglecting the source term, a plane-wave analysis of the elastic anisotropic wave equation yields the Christoffel equation,

$$\widetilde{\mathbf{\Gamma}}\widetilde{\mathbf{u}} = \rho\omega^2\widetilde{\mathbf{u}}, \tag{5}$$

or

$$(\widetilde{\mathbf{\Gamma}} - \rho\omega^2\mathbf{I})\widetilde{\mathbf{u}} = \mathbf{0}, \tag{6}$$

where ω is the frequency, $\widetilde{\mathbf{u}} = (\widetilde{u}_x, \widetilde{u}_y, \widetilde{u}_z)^T$ is the wavefield in Fourier domain, $\widetilde{\Gamma} = \widetilde{\mathbf{L}}\mathbf{C}\widetilde{\mathbf{L}}^T$ is the symmetric Christoffel matrix, $\mathbf{I}$ is a 3×3 identity matrix. To support the sign notation in equations 5 and 6, we remove the imaginary unit i of the wavenumber-domain counterpart of the gradient operator $\bigtriangledown$ and thus express matrix $\widetilde{\mathbf{L}}$ as:

$$\widetilde{\mathbf{L}} = \begin{pmatrix} k_x & 0 & 0 & 0 & k_z & k_y \\ 0 & k_y & 0 & k_z & 0 & k_x \\ 0 & 0 & k_z & k_y & k_x & 0 \end{pmatrix}. \tag{7}$$

Setting the determinant of $\widetilde{\mathbf{\Gamma}} - \rho\omega^2\mathbf{I}$ in equation 6 to zero gives the characteristic equation, and expanding that determinant gives the (angular) dispersion relation.

For a given spatial direction specified by a wave vector $\mathbf{k} = (k_x, k_y, k_z)^T$, the characteristic equation poses a standard 3×3 eigenvalue problem. The three eigenvalues correspond to the phase velocities of the qP-wave and two qS waves. Inserting one of the eigenvalues back into the Christoffel equation gives ratios of the components of $\widetilde{\mathbf{u}}$, from which the polarization or displacement direction can be determined for the given wave mode. In general, these directions are neither parallel nor perpendicular to the wave vector, and depend on the local material parameters for the anisotropic medium. For a given wave vector or slowness direction, the polarization vectors of the three wave modes are always mutually orthogonal.

Applying an inverse Fourier transform to the dispersion relation yields a high-order PDE in time and space and contains mixed space and time derivatives. Setting the shear velocity along the axis of symmetry to zero while using Thomsen's parameter notation yields the pseudo-acoustic dispersion relation and wave equation in VTI media (Alkhalifah, 2000). Most published methods instead have used coupled PDEs (derived from the pseudo-acoustic dispersion relation) that are only second-order in time and eliminate the mixed space-time derivatives, e.g., Zhou et al. (2006b). Many kinematically equivalent coupled second-order systems can be generated from the dispersion relation by similarity transformations (Fowler et al., 2010). In the next section, we present a particular similarity transformation to the Christoffel equation in order to derive a minimal second-order coupled system, which is helpful for simulating propagation of separated qP-waves in anisotropic media.

Pseudo-pure-mode qP-wave equation

To describe propagation of separated qP-waves in anisotropic media, we first revisit the classical wave mode separation theory. In isotropic media, scalar P-wave can be separated from the extrapolated vector wavefield $\mathbf{u}$ by applying a divergence operation: $P = \bigtriangledown \cdot \mathbf{u}$. In the wavenumber domain, this can be equivalently expressed as a dot product that essentially projects the wavefield $\widetilde{\mathbf{u}}$ onto the wave vector $\mathbf{k}$, i.e.,

$$\widetilde{P} = i\mathbf{k} \cdot \widetilde{\mathbf{u}}, \tag{8}$$

Similarly, for an anisotropic medium, scalar qP-waves can be separated by projecting the vector wavefields onto the true polarization directions of qP-waves by (Dellinger and Etgen, 1990),

$$q\widetilde{P} = i\mathbf{a_p} \cdot \widetilde{\mathbf{u}}, \tag{9}$$

where $\mathbf{a}_p = (a_{px}, a_{py}, a_{pz})^T$ represents the polarization vector for qP-waves. For heterogeneous models, this scalar projection can be performed using nonstationary spatial filtering depending on local material parameters (Yan and Sava, 2009).

To provide more flexibility for characterizing wave propagation in anisotropic media, we suggest to split the one-step projection into two steps, of which the first step implicitly implements partail wave mode separation (like in equation 8) during wavefield extrapolation with a transformed wave equation, while the second step is

designed to correct the projection deviation implied by equations 8 and 9. We achieve this on the base of the following observations: the difference of the polarization between an ordinary anisotropic medium and its isotropic reference at a given wave vector direction is usually small, though exceptions are possible (Thomsen, 1986; Tsvankin and Chesnokov, 1990); The wave vector can be taken as the isotropic reference of the polarization vector for qP-waves; It is a material-independent operation to project the elastic wavefield onto the wave vector.

Therefore, we introduce a similarity transformation to the Christoffel matrix, i.e.,

$$\widetilde{\overline{\mathbf{\Gamma}}} = \mathbf{M_p}\widetilde{\mathbf{\Gamma}}{\mathbf{M_p}}^{-1}, \tag{10}$$

with a invertible 3×3 matrix $\mathbf{M}_p$ related to the wave vector:

$$\mathbf{M_p} = \begin{pmatrix} ik_x & 0 & 0 \\ 0 & ik_y & 0 \\ 0 & 0 & ik_z \end{pmatrix}. \tag{11}$$

Accordingly, we derive an equivalent Christoffel equation,

$$\widetilde{\overline{\mathbf{\Gamma}}}\widetilde{\overline{\mathbf{u}}} = \rho\omega^2\widetilde{\overline{\mathbf{u}}}, \tag{12}$$

for a transformed wavefield:

$$\widetilde{\overline{\mathbf{u}}} = \mathbf{M_p}\widetilde{\mathbf{u}}. \tag{13}$$

The above similarity transformation does not change the eigeinvalues of the Christoffel matrix and thus introduces no kinematic errors for the wavefields. By the way, we can obtain the same transformed Christoffel equation if matrix $\mathbf{M}_p$ is constructed using the normalized wavenumbers to ensure all spatial frequencies are uniformly scaled. For a locally smooth medium, applying an inverse Fourier transform to equation 12, we obtain a coupled linear second-order system kinematically equivalent to the original elastic wave equation:

$$\rho\frac{\partial^2\overline{\mathbf{u}}}{\partial t^2} = \overline{\mathbf{\Gamma}}\overline{\mathbf{u}}, \tag{14}$$

where $\overline{\mathbf{u}}$ represents the time-space domain wavefields, and $\overline{\mathbf{\Gamma}}$ represents the Christoffel differential-operator matrix after the similarity transformation.

For the transformed elastic wavefield in the wavenumber-domain, we have

$$\widetilde{\overline{u}} = \widetilde{\overline{u}}_x + \widetilde{\overline{u}}_y + \widetilde{\overline{u}}_z = i\mathbf{k}\cdot\widetilde{\mathbf{u}}. \tag{15}$$

And in space-domain, we also have

$$\overline{u} = \overline{u}_x + \overline{u}_y + \overline{u}_z = \bigtriangledown\cdot\mathbf{u}, \tag{16}$$

with

$$\overline{u}_x = \frac{\partial u_x}{\partial x}, \qquad \overline{u}_y = \frac{\partial u_y}{\partial y}, \qquad \text{and} \qquad \overline{u}_z = \frac{\partial u_z}{\partial z}. \tag{17}$$

These imply that the new wavefield components essentially represent the spatial derivatives of the original components of the displacement wavefield, and the transformation (equation 13) plus the summation of the transformed wavefield components (like in equation 15 or 16) essentially finishes a scalar projection of the displacement wavefield onto the wave vector. For isotropic media, such a projection directly produces scalar P-wave data. In an anisotropic medium, however, only a partial wave-mode separation is achieved becuase there is usually a direction deviation between the wave vector and the polarization vector of qP-wave. Generally, this deviation turns out to be small and its maximum value rarely exceeds 20° for typical anisotropic earth media(Psencik and Gajewski, 1998). Because of the orthognality of qP- and qS-wave polarizations, the projection deviations of qP-waves are generally far less than those of the qSV-waves when the elastic wavefields are projected onto the isotropic references of the qP-wave's polarization vectors. As demonstrated in the synthetic examples of various symmetry and strength of anisotropy, the scalar wavefield $\overline{u}$ represents dominantly the energy of qP-waves but contains some weak residual qS-waves. This is why we call the coupled system (equation 14) a pseudo-pure-mode wave equation for qP-wave in anisotropic media.

Substituting the corresponding stiffness matrix into the above derivations, we get the extended expression of pseudo-pure-mode qP-wave equation for any anisotropic media. As demonstrated in Appendix A, pseudo-pure-mode qP-wave equation in vertical TI and orthorhombic media can be expressed as

$$\begin{aligned}
\rho\frac{\partial^2\overline{u}_x}{\partial t^2} &= C_{11}\frac{\partial^2\overline{u}_x}{\partial x^2} + C_{66}\frac{\partial^2\overline{u}_x}{\partial y^2} + C_{55}\frac{\partial^2\overline{u}_x}{\partial z^2} + (C_{12}+C_{66})\frac{\partial^2\overline{u}_y}{\partial x^2} + (C_{13}+C_{55})\frac{\partial^2\overline{u}_z}{\partial x^2},\\
\rho\frac{\partial^2\overline{u}_y}{\partial t^2} &= C_{66}\frac{\partial^2\overline{u}_y}{\partial x^2} + C_{22}\frac{\partial^2\overline{u}_y}{\partial y^2} + C_{44}\frac{\partial^2\overline{u}_y}{\partial z^2} + (C_{12}+C_{66})\frac{\partial^2\overline{u}_x}{\partial y^2} + (C_{23}+C_{44})\frac{\partial^2\overline{u}_z}{\partial y^2},\\
\rho\frac{\partial^2\overline{u}_z}{\partial t^2} &= C_{55}\frac{\partial^2\overline{u}_z}{\partial x^2} + C_{44}\frac{\partial^2\overline{u}_z}{\partial y^2} + C_{33}\frac{\partial^2\overline{u}_z}{\partial z^2} + (C_{13}+C_{55})\frac{\partial^2\overline{u}_x}{\partial z^2} + (C_{23}+C_{44})\frac{\partial^2\overline{u}_y}{\partial z^2}.
\end{aligned} \tag{18}$$

Note that, unlike the original elastic wave equation, pseudo-pure-mode wave equation dose not contain mixed partial derivatives. This is a good news because it takes more computational cost to compute the mixed partial derivatives using a finite-difference algorithm with required accuracy. In the forthcoming text, we focus on demonstration of pseudo-pure-mode qP-wave equations for TI media while briefly supplement similar derivation for orthorhombic media in Appendix B.

Pseudo-pure-mode qP-wave equation in VTI media

For a VTI medium, there are only five independent parameters: C_{11}, C_{33}, C_{44}, C_{66} and C_{13}, with $C_{12} = C_{11} - 2C_{66}$, $C_{22} = C_{11}$, $C_{23} = C_{13}$ and $C_{55} = C_{44}$. So we rewrite

equation 18 as,

$$\begin{aligned}
\rho\frac{\partial^2\overline{u}_x}{\partial t^2} &= C_{11}\frac{\partial^2\overline{u}_x}{\partial x^2} + C_{66}\frac{\partial^2\overline{u}_x}{\partial y^2} + C_{44}\frac{\partial^2\overline{u}_x}{\partial z^2} + (C_{11}-C_{66})\frac{\partial^2\overline{u}_y}{\partial x^2} + (C_{13}+C_{44})\frac{\partial^2\overline{u}_z}{\partial x^2},\\
\rho\frac{\partial^2\overline{u}_y}{\partial t^2} &= C_{66}\frac{\partial^2\overline{u}_y}{\partial x^2} + C_{11}\frac{\partial^2\overline{u}_y}{\partial y^2} + C_{44}\frac{\partial^2\overline{u}_y}{\partial z^2} + (C_{11}-C_{66})\frac{\partial^2\overline{u}_x}{\partial y^2} + (C_{13}+C_{44})\frac{\partial^2\overline{u}_z}{\partial y^2},\\
\rho\frac{\partial^2\overline{u}_z}{\partial t^2} &= C_{44}\frac{\partial^2\overline{u}_z}{\partial x^2} + C_{44}\frac{\partial^2\overline{u}_z}{\partial y^2} + C_{33}\frac{\partial^2\overline{u}_z}{\partial z^2} + (C_{13}+C_{44})\frac{\partial^2\overline{u}_x}{\partial z^2} + (C_{13}+C_{44})\frac{\partial^2\overline{u}_y}{\partial z^2}.
\end{aligned} \tag{19}$$

Since a TI material has cylindrical symmetry in its elastic properties, it is safe to sum the first two equations in equation 19 to yield a simplified form for wavefield modeling and RTM, namely

$$\begin{aligned}
\rho\frac{\partial^2\overline{u}_{xy}}{\partial t^2} &= C_{11}(\frac{\partial^2}{\partial x^2}+\frac{\partial^2}{\partial y^2})\overline{u}_{xy} + C_{44}\frac{\partial^2\overline{u}_{xy}}{\partial z^2} + (C_{13}+C_{44})(\frac{\partial^2}{\partial x^2}+\frac{\partial^2}{\partial y^2})\overline{u}_z,\\
\rho\frac{\partial^2\overline{u}_z}{\partial t^2} &= C_{44}(\frac{\partial^2}{\partial x^2}+\frac{\partial^2}{\partial y^2})\overline{u}_z + C_{33}\frac{\partial^2\overline{u}_z}{\partial z^2} + (C_{13}+C_{44})\frac{\partial^2\overline{u}_{xy}}{\partial z^2},
\end{aligned} \tag{20}$$

where $\overline{u}_{xy} = \overline{u}_x + \overline{u}_y$ represents the sum of the two horizontal components. Pure SH-waves horizontally polarize in the isotropic planes of VTI media with the polarization given by $(-k_y, k_x, 0)$, which implies $ik_x\widetilde{u}_x + ik_y\widetilde{u}_y = 0$, i.e., $\overline{u}_{xy} = 0$, for the SH-wave. Therefore, the above partial summation (after the first-step projection) completes divergence operation and removes the SH-waves from the three-component pseudo-pure-mode qP-wave fields. As a result, there are no terms related to C_{66} any more in equation 20. Compared with original elastic wave equation, equation 20 further reduces the compuational costs for 3D wavefield modeling and RTM for VTI media.

Applying the Thomsen notation (Thomsen, 1986),

$$\begin{aligned}
C_{11} &= (1+2\epsilon)\rho v_{p0}^2,\\
C_{33} &= \rho v_{p0}^2,\\
C_{44} &= \rho v_{s0}^2,\\
(C_{13}+C_{44})^2 &= \rho^2(v_{p0}^2 - v_{s0}^2)(v_{pn}^2 - v_{s0}^2),
\end{aligned} \tag{21}$$

the pseudo-pure-mode qP-wave equation can be expressed as,

$$\begin{aligned}
\frac{\partial^2\overline{u}_{xy}}{\partial t^2} &= v_{px}^2(\frac{\partial^2}{\partial x^2}+\frac{\partial^2}{\partial y^2})\overline{u}_{xy} + v_{s0}^2\frac{\partial^2\overline{u}_{xy}}{\partial z^2} + \sqrt{(v_{p0}^2 - v_{s0}^2)(v_{pn}^2 - v_{s0}^2)}(\frac{\partial^2}{\partial x^2}+\frac{\partial^2}{\partial y^2})\overline{u}_z,\\
\frac{\partial^2\overline{u}_z}{\partial t^2} &= v_{s0}^2(\frac{\partial^2}{\partial x^2}+\frac{\partial^2}{\partial y^2})\overline{u}_z + v_{p0}^2\frac{\partial^2\overline{u}_z}{\partial z^2} + \sqrt{(v_{p0}^2 - v_{s0}^2)(v_{pn}^2 - v_{s0}^2)}\frac{\partial^2\overline{u}_{xy}}{\partial z^2},
\end{aligned} \tag{22}$$

where v_{p0} and v_{s0} represent the vertical velocities of qP- and qSV-waves, $v_{pn} = v_{p0}\sqrt{1+2\delta}$ represents the interval NMO velocity, $v_{px} = v_{p0}\sqrt{1+2\epsilon}$ represents the horizontal velocity of qP-waves, δ and ϵ are the other two Thomsen coefficients. Unlike other coupled second-order systems derived from the dispersion relation of VTI

media (Zhou et al., 2006b), the wavefield components in equations 20 and 22 have clear physical meaning and their summation automatically produces scalar wavefields dominant of qP-wave energy. Equation 22 is also similar to a minimal coupled system (equation 30 in their paper) demonstrated by Fowler et al. (2010), except that it is now derived from a significant similarity transformation that helps to enhance qP-waves and suppress qS-waves (after summing the transformed wavefield components). This is undoubtedly useful for migration of conventional seismic data representing mainly qP-wave data.

We can also obtain a pseudo-acoustic coupled system by setting $v_{s0} = 0$ in equation 22, namely:

$$\begin{aligned} \frac{\partial^2 \overline{u}_{xy}}{\partial t^2} &= (1+2\epsilon) v_{p0}^2 (\frac{\partial^2}{\partial x^2} + \frac{\partial^2}{\partial y^2}) \overline{u}_{xy} + \sqrt{1+2\delta} v_{p0}^2 (\frac{\partial^2}{\partial x^2} + \frac{\partial^2}{\partial y^2}) \overline{u}_z, \\ \frac{\partial^2 \overline{u}_z}{\partial t^2} &= v_{p0}^2 \frac{\partial^2 \overline{u}_z}{\partial z^2} + \sqrt{1+2\delta} v_{p0}^2 \frac{\partial^2 \overline{u}_{xy}}{\partial z^2}. \end{aligned} \tag{23}$$

The pseudo-acoustic approximation does not significantly affect the kinematic signatures but may distort the reflection, transmission and conversion coefficients (thus the amplitudes) of waves in elastic media.

If we further apply the isotropic assumption (seting $\delta = 0$ and $\epsilon = 0$) and sum the two equations in equation 23, we get the familar constant-density acoustic wave equation:

$$\frac{\partial^2 \overline{u}}{\partial t^2} = v_p^2 (\frac{\partial^2}{\partial x^2} + \frac{\partial^2}{\partial y^2} + \frac{\partial^2}{\partial z^2}) \overline{u}, \tag{24}$$

where $\overline{u} = \overline{u}_{xy} + \overline{u}_z$ represents the acoustic pressure wavefield, and v_p is the propagation velocity of isotropic P-wave.

Pseudo-pure-mode qP-wave equation in TTI media

In the case of transversely isotropic media with a tilted symmetry axis, the elastic tensor loses its simple form. Written in Voigt notation, it contains nonzero entries in all four quadrants if expressed in global Cartesian coordinates $\mathbf{x} = (x, y, z)$. The generalization of pseudo-pure-mode wave equation to a tilted symmetry axis involves no additional physics but greatly complicates the algebra. One strategy to derive the wave equations in TTI media is to locally rotate the coordinate system so that its third axis coincides with the symmetry axis, and make use of the simple form in VTI media.

We introduce a transformation to a rotated coordinate system $\widehat{\mathbf{x}} = (\widehat{x}, \widehat{y}, \widehat{z})$,

$$\widehat{\mathbf{x}} = \mathbf{R}^T \mathbf{x}, \tag{25}$$

where the rotation matrix $\mathbf{R}$ is dependent on the tilt angle θ and the azimuth φ of

the symmetry axis, namely,

$$\mathbf{R} = \begin{pmatrix} r_{11} & r_{12} & r_{13} \\ r_{21} & r_{22} & r_{23} \\ r_{31} & r_{32} & r_{33} \end{pmatrix} = \begin{pmatrix} \cos\varphi & -\sin\varphi & 0 \\ \sin\varphi & \cos\varphi & 0 \\ 0 & 0 & 1 \end{pmatrix} \begin{pmatrix} \cos\theta & 0 & -\sin\theta \\ 0 & 1 & 0 \\ \sin\theta & 0 & \cos\theta \end{pmatrix}. \tag{26}$$

So,

$$\begin{aligned} r_{11} &= \cos\theta\cos\varphi, \\ r_{12} &= -\sin\varphi, \\ r_{13} &= -\sin\theta\cos\varphi, \\ r_{21} &= \cos\theta\sin\varphi, \\ r_{22} &= \cos\varphi, \\ r_{23} &= -\sin\theta\sin\varphi, \\ r_{31} &= \sin\theta, \\ r_{32} &= 0, \\ r_{33} &= \cos\theta. \end{aligned} \tag{27}$$

Assuming that the rotation operator $\mathbf{R}$ varies slowly so that its spatial derivatives can be ignored, the second-order differential operators in the rotated coordinate system aligned with the symmetry axis are given as:

$$\begin{aligned} \frac{\partial^2}{\partial\widehat{x}^2} &= r_{11}^2\frac{\partial^2}{\partial x^2} + r_{21}^2\frac{\partial^2}{\partial y^2} + r_{31}^2\frac{\partial^2}{\partial z^2} + 2r_{11}r_{21}\frac{\partial^2}{\partial x\partial y} + 2r_{11}r_{31}\frac{\partial^2}{\partial x\partial z} + 2r_{21}r_{31}\frac{\partial^2}{\partial y\partial z}, \\ \frac{\partial^2}{\partial\widehat{y}^2} &= r_{12}^2\frac{\partial^2}{\partial x^2} + r_{22}^2\frac{\partial^2}{\partial y^2} + r_{32}^2\frac{\partial^2}{\partial z^2} + 2r_{12}r_{22}\frac{\partial^2}{\partial x\partial y} + 2r_{12}r_{32}\frac{\partial^2}{\partial x\partial z} + 2r_{22}r_{32}\frac{\partial^2}{\partial y\partial z}, \\ \frac{\partial^2}{\partial\widehat{z}^2} &= r_{13}^2\frac{\partial^2}{\partial x^2} + r_{23}^2\frac{\partial^2}{\partial y^2} + r_{33}^2\frac{\partial^2}{\partial z^2} + 2r_{13}r_{23}\frac{\partial^2}{\partial x\partial y} + 2r_{13}r_{33}\frac{\partial^2}{\partial x\partial z} + 2r_{23}r_{33}\frac{\partial^2}{\partial y\partial z}. \end{aligned} \tag{28}$$

Substituting these differential operators into the pseudo-pure-mode qP-wave equation of VTI media yields the pseudo-pure-mode qP-wave equation for TTI media in the global Cartesian coordinates. Likewise, the pseudo-pure-mode qP-wave equation in TTI media can be further simplified by applying the pseudo-acoustic approximation. We must mention that, the above coordinate rotation in deriving the wave equations for TTI and tilted orthorhombic media (see Appendix B) should be improved to enhance numerical stability according to some significant insights provided in recent literatures (Duveneck and Bakker, 2011; Macesanu, 2011; Zhang et al., 2011; Bube et al., 2012).

CORRECTION OF PROJECTION DEVIATION TO REMOVE QS-WAVES

According to the theory of wave mode separation in anisotropic media, one needs to project the elastic wavefields onto the polarization direction to get the separated

wavefields of the given mode (Dellinger and Etgen, 1990). Mathematically, this can be implemented through a dot product of the original vector wavefields and the polarization vector in the wavenumber domain (Dellinger and Etgen, 1990) or applying pseudo-derivative operators to the vector wavefields in the space-domain (Yan and Sava, 2009). However, the pseudo-pure-mode qP-wave equations are derived by a similarity transformation aiming to project the displacement wavefield onto the isotropic reference of qP-wave's polarization vector. A partial mode separation has been automatically achieved during wavefield extrapolation using the pseudo-pure-mode qP-wave equations. For typical anisotropic earth media, thanks to the small departure of qP-wave's polarization direction from its isotropic reference, the resulting pseudo-pure-mode wavefields are dominated by qP-wave energy and contaminated by residual qS-waves. To achieve a complete mode separation, we should further correct the projection deviations resulting from the differences between polarization and its isotropic reference. In other words, we split the conventional one-step wave mode separation for anisotropic media (Dellinger and Etgen, 1990; Yan and Sava, 2009) into two steps, of which the first one is implicitly achieved during extrapolating the pseudo-pure-mode wavefields and the second one is implemented after that using the approach that we will present immediately.

Taking VTI as an example, the deviation angle ζ between the polarization and propagation directions has a complicated nonlinear relation with anisotropic parameters and the phase angle (see Appendix C). According to its expression for weak anisotropic VTI media (Rommel, 1994; Tsvankin, 2001), it seems that the deviation is mainly affected by the difference between ϵ and δ, the magnitude of δ (when $\epsilon - \delta$ stays the same) and the ratio of vertical velocities of qP- and qS-wave, as well as the phase angle. It is possible to design a filtering algorithm to suppress the residual qS-waves using the deviation angle given under the assumption of weak anisotropy. To completely remove the residual qS-waves and correctly separate the qP-waves for arbitrary anisotropy, we propose an accurate correction approach according to the deviation between polarization and wave vectors.

Considering equations 8, 9, 13, and 15, we first decompose the polarization vector of qP-wave $\mathbf{a}_p$ as follows:

$$\mathbf{a}_p = \mathbf{E}_p \mathbf{k}, \tag{29}$$

where the deviation operator satisfies,

$$\mathbf{E}_p = \begin{pmatrix} \frac{a_{px}}{k_x} & 0 & 0 \\ 0 & \frac{a_{py}}{k_y} & 0 \\ 0 & 0 & \frac{a_{pz}}{k_z} \end{pmatrix}. \tag{30}$$

This matrix can be constructed once the qP-wave polarization directions are determined based on the local medium properties at a grid point. For TI media, there are analytical expressions for the qP-wave polarization vectors (Dellinger, 1991). For other anisotropic media with lower symmetry (such as orthorhombic media), we have to numerically compute the polarization vectors using the Christoffel equation.

Then we correct the pseudo-pure-mode qP-wave fields $\widetilde{\overline{\mathbf{u}}} = (\widetilde{\overline{u}}_x, \widetilde{\overline{u}}_y, \widetilde{\overline{u}}_z)^T$ using a wavenumber-domain filtering based on the deviation operator:

$$\widetilde{\mathbf{u}}_p = \mathbf{E}_p \cdot \widetilde{\overline{\mathbf{u}}}, \tag{31}$$

and finally extract the scalar qP-wave data using

$$u_p = u_{px} + u_{py} + u_{pz} \tag{32}$$

after 3D inverse Fourier transforms. Here, the magnitude of the deviation operator for a certain wavenumber $k = \sqrt{k_x^2 + k_y^2 + k_z^2}$ is a constant becuase this operator is computed by using the normalized wave and polarization vectors in equation 30. This ensures that for a certain wavenumber, the separated qP-waves are uniformly scaled. More important, this correction step thoroughly removes the residual qS-wave energy.

In heterogeneous anisotropic media, the polarization directions and thus the deviation operators vary spatially, depending on the local material parameters. To account for spatial variability, we propose an equivalent expression to equations 31 and 32 as a nonstationary filtering in the space domain at each location,

$$u_p = E_{px}(\overline{u}_x) + E_{py}(\overline{u}_y) + E_{pz}(\overline{u}_z) \tag{33}$$

where the pseudo-derivative operators $E_{px}(\cdot)$, $E_{py}(\cdot)$, and $E_{pz}(\cdot)$ represent the inverse Fourier transforms of the diagonal elements in the deviation matrix $\mathbf{E}_p$.

Figure 1 displays the wavenumber-domain operators of projection onto isotropic (reference) and anisotropic polarization vectors (namely $\mathbf{k}$ and $\mathbf{a}_p$) as well as the corresponding deviation operator $\mathbf{E}_p$ for a 2D homogeneous VTI medium with $v_{p0} = 3000m/s$, $v_{s0} = 1500m/s$, $\epsilon = 0.25$ and $\delta = -0.25$. Note that $\mathbf{E}_p$ is not simply the difference between $\mathbf{k}$ and $\mathbf{a}_p$, and $\mathbf{E}_p$ becomes the identity operator in case of an isotropic medium. In the space-domain, projecting onto isotropic polarization directions is equivalent to a divergence operation using partial derivative operators, while projection onto polarization directions of qP-waves use operators that have the character of pseudo-derivative operators, due to anisotropy (see Figure 2). Figure 3 shows that the variation of the anisotropy changes the deviation operators greatly. The weaker the anisotropy, the more compact the deviation operators appear. The observation is basically consistent with the equation of polarization deviation angle for VTI media with weak anisotropy. The exact pseudo-derivative operators are very long series in the discretized space domain. Generally, the far ends of these operators have ignorable values even for strong anisotropy. Therefore, in practice, we could truncate the operators to make the spatial filters short and computationally efficient.

This procedure to separate qP-waves, although accurate, is computationally expensive, especially in 3D heterogeneous media. Like the computational problem in conventional wave mode separation from the anisotropic elastic wavefields (Yan and Sava, 2009, 2012), the spatial filtering to separate qP-waves is significantly more expensive than extrapolating the pseudo-pure-mode wavefields. In practice, we find that it is not necessary to apply the filtering at every time step. A larger time interval is

allowed to save costs enormously, especially for RTM of multi-shot seismic data. According to our experiments, there is little difference between the two migrated images when the filtering is applied at every one and two time step (if only the filtered wavefields are used in the imaging procedure), although about three-forth of the original computational cost are saved for the filtering in the latter case. Moreover, filtering at every three time step still produces an acceptable migrated image. We may further improve the efficiency of the filtering procedure by using the algorithm that resembles the phase-shift plus interpolation (PSPI) scheme recently used in anisotropic wave mode separation (Yan and Sava, 2011). Alternatively, we may greatly reduce the compuational cost but guarantee the accuracy using the mixed (space-wavenumber) domain filtering algorithm based on low-rank approximation (Cheng and Fomel, 2013).

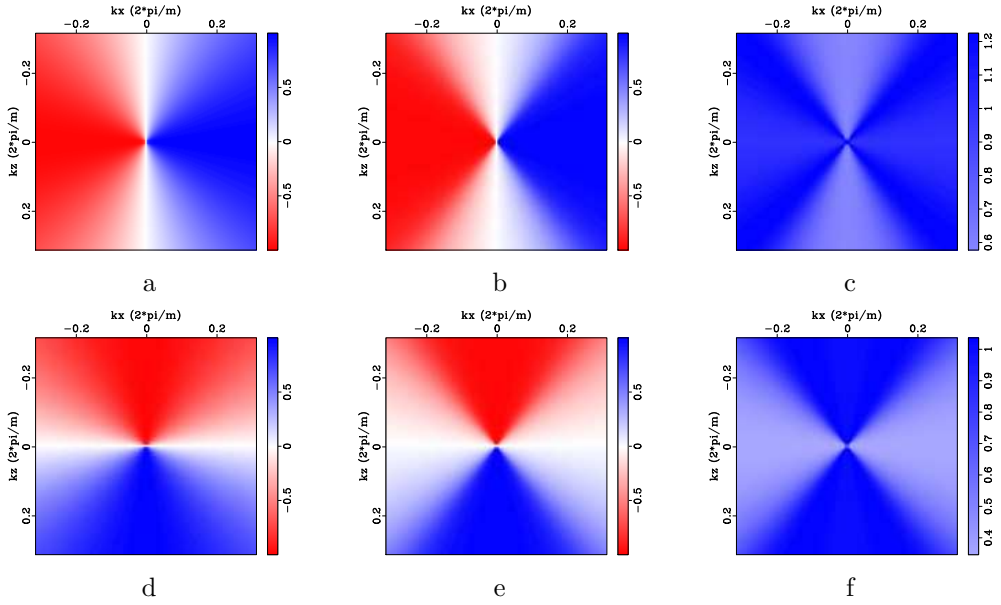

Figure 1: Normalized wavenumber-domain operators of projection onto isotropic (reference) and anisotropic polarization vectors of qP-waves, and wavenumber-domain deviation operators in a 2D homogeneous VTI medium: $\mathbf{k}$ (left), $\mathbf{a}_p$ (middle) and $\mathbf{E}_p$ (right); Top: x-component, Bottom: z-component.

In kinematics, it seems that we can extract scalar qSV-wave fields from the pseudo-pure-mode qP-wave fields $\overline{\mathbf{u}}$ by filtering according to the projection deviation defined by qSV-wave's polarization and wave vector. However, unlike separation of the qP-wave mode, the large projection deviations for qSV-wave modes would result in significant discontinuities in the wavenumber-domain correction operators and strong tails extending off to infinity in the space domain. Accordingly, this reduces compactness of the spatial filters, which prohibits applying the same truncation as for qP-wave spatial filters to reduce computational cost. Computational tricks such as smoothing may result in distorted and imcomplete separation. That is why we are developing a similar approach to simulate propagation of separated qS-wave modes based on their own pseudo-pure-mode wave equations and the corresponding projection deviation corrections for anisotropic media (Kang and Cheng, 2012).

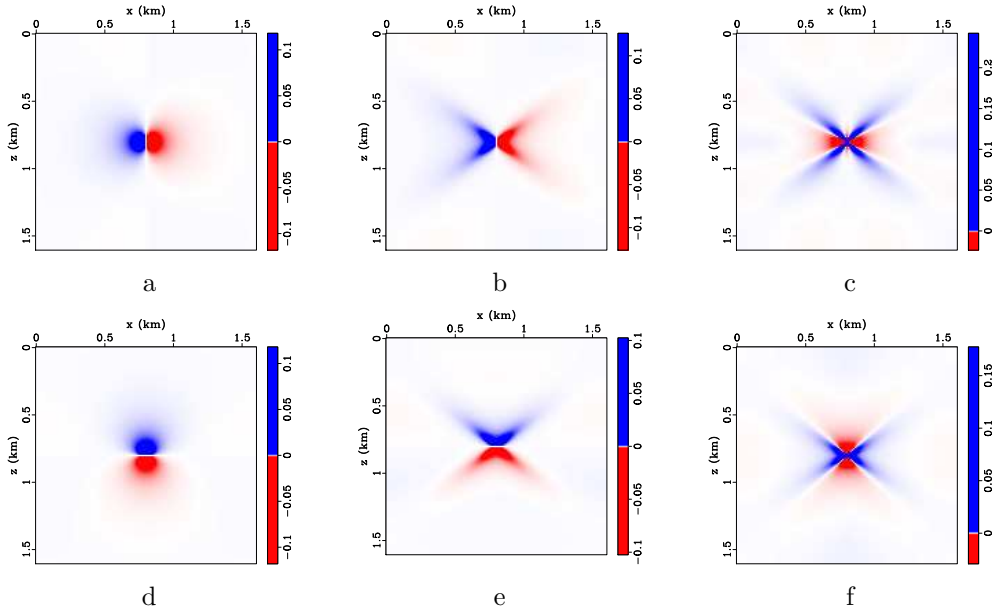

Figure 2: Space-domain operators of projecting onto isotropic (left) and anisotropic (middle) polarization vectors, and the corresponding deviation operators (right): Top: x-component, Bottom: z-component. Note that the operators are tapered before transforming into space-domain and the same gain is applied to all pictures to highlight the differences among these operators.

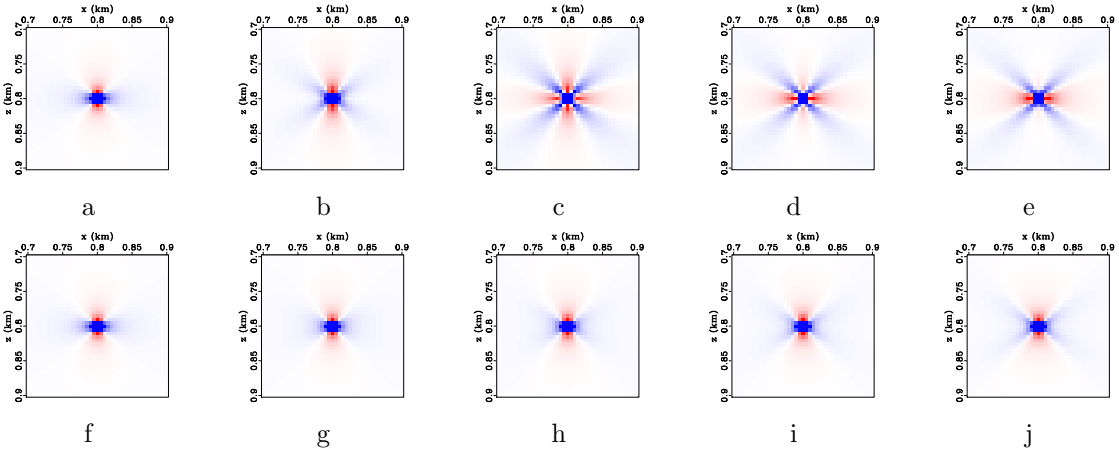

Figure 3: Comparison of the spatial domain deviation operators in VTI media with varied anisotropy strength: In all cases, $v_{p0} = 3000m/s$, $v_{s0} = 1500m/s$, and ϵ is fixed as 0.2. From left to right, δ is set as 0.2, 0.1, 0, -0.1, and -0.2, respectively. Top: x-components; Bottom: z-components. To highlight the differences,the same gain is applied to all pictures.

EXAMPLES

1. Simulating propagation of separated wave modes

1.1 Homogeneous VTI model

For comparison, we first appply the original anisotropic elastic wave equation to synthesize wavefields in a homogeneous VTI medium with weak anisotropy, in which $v_{p0} = 3000m/s$, $v_{s0} = 1500m/s$, $\epsilon = 0.1$, and $\delta = 0.05$. Figure 4a and 4b display the horizontal and vertical components of the displacement wavefields at 0.3 s. Then we try to simulate propagation of separated wave modes using the pseudo-pure-mode qP-wave equation (equation 22 in its 2D form). Figure 4c and 4d display the two components of the pseudo-pure-mode qP-wave fields, and Figure 4e displays their summation, i.e., the pseudo-pure-mode scalar qP-wave fields with weak residual qSV-wave energy. Compared with the theoretical wavefront curves (see Figure 4f) calculated on the base of group velocities and angles, pseudo-pure-mode scalar qP-wave fields have correct kinematics for both qP- and qSV-waves. We finally remove residual qSV-waves and get completely separated scalar qP-wave fields by applying the filtering to correct the projection deviation (Figure 4g).

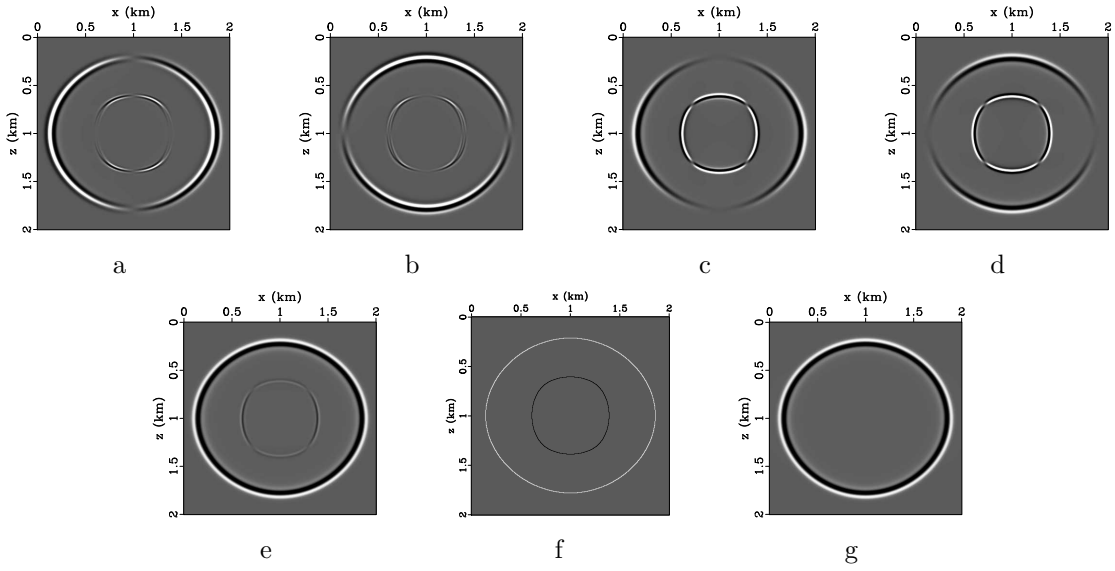

Figure 4: Synthesized wavefields in a VTI medium with weak anisotropy: (a) x- and (b) z-components synthesized by original elastic wave equation; (c) x- and (d) z-components synthesized by pseudo-pure-mode qP-wave equation; (e) pseudo-pure-mode scalar qP-wave fields; (f) kinematics of qP- and qSV-waves; and (g) separated scalar qP-wave fields.

Then we consider wavefield modeling in a homogeneous VTI medium with strong anisotropy, in which $v_{p0} = 3000m/s$, $v_{s0} = 1500m/s$, $\epsilon = 0.25$, and $\delta = -0.25$. Figure 5 displays the wavefield snapshots at 0.3 s synthesized by using original elastic wave equation and pseudo-pure-mode qP-wave equation respectively. Note that

the pseudo-pure-mode qP-wave fields still accurately represent the qP- and qSV-waves' kinematics. Although the residual qSV-wave energy becomes stronger when the strength of anisotropy increases, the filtering step still removes these residual qSV-waves effectively.

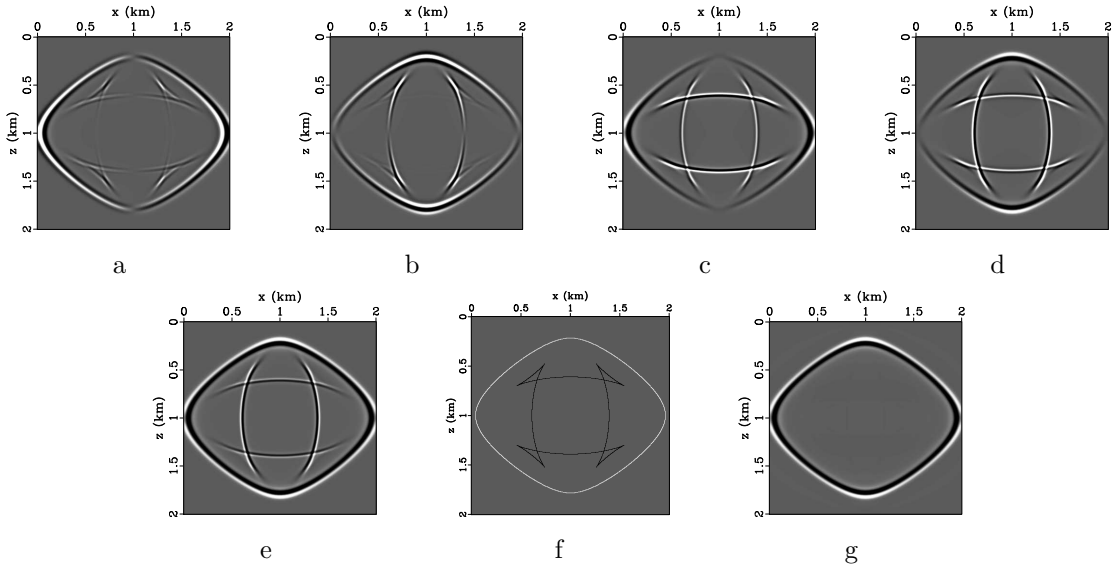

Figure 5: Synthesized wavefields in a VTI medium with strong anisotropy: (a) x- and (b) z-components synthesized by original elastic wave equation; (c) x- and (d) z-components synthesized by pseudo-pure-mode qP-wave equation; (e) pseudo-pure-mode scalar qP-wave fields; (f) kinematics of qP- and qSV-waves; and (g) separated scalar qP-wave fields.

1.2 Two-layer TI model

This example demonstrates the approach on a two-layer TI model, in which the first layer is a very strong VTI medium with $v_{p0} = 2500m/s$, $v_{s0} = 1200m/s$, $\epsilon = 0.25$, and $\delta = -0.25$, and the second layer is a TTI medium with $v_{p0} = 3600m/s$, $v_{s0} = 1800m/s$, $\epsilon = 0.2$, $\delta = 0.1$, and $\theta = 30°$. The horizontal interface between the two layers is positioned at a depth of 1.167 km. Figure 6a and 6d display the horizontal and vertical components of the displacement wavefields at 0.3 s. Using the pseudo-pure-mode qP-wave equation, we simulate equivalent wavefields on the same model. Figure 6b and 6e display the two components of the pseudo-pure-mode qP-wave fields at the same time step. Figure 6c and 6f display pseudo-pure-mode scalar qP-wave fields and separated qP-wave fields respectively. Obviously, residual qSV-waves (including transmmited, reflected and converted qSV-waves) are effectively removed, and all transmitted, reflected as well as converted qP-waves are accurately separated after the projection deviation correction.

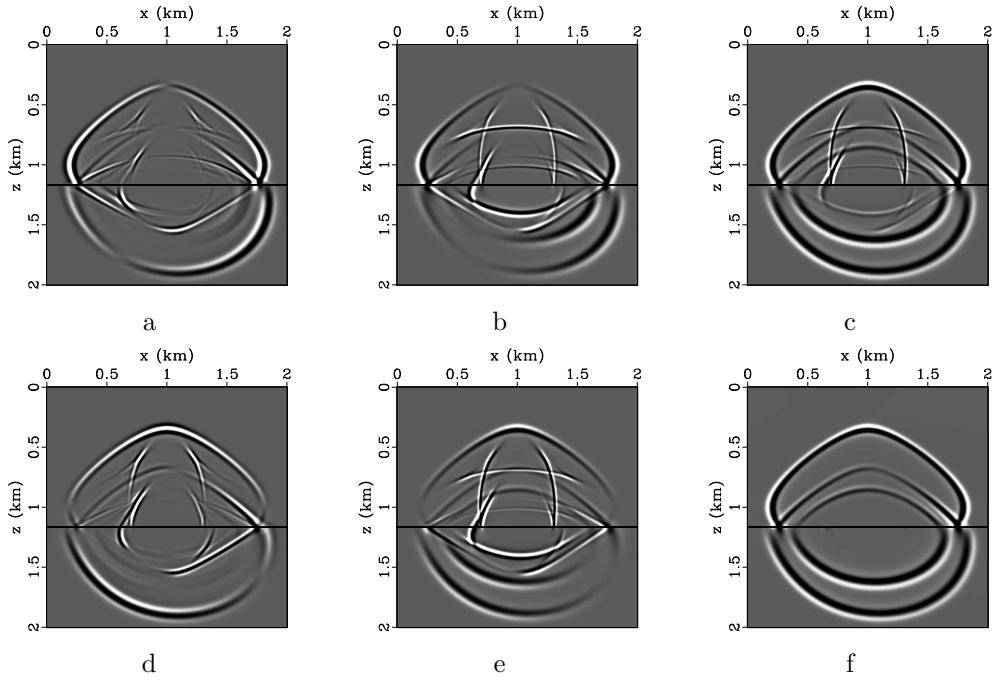

Figure 6: Synthesized wavefields on a two-layer TI model with strong anisotropy in the first layer and a tilted symmetry axis in the second layer: (a) x- and (d) z-components synthesized by original elastic wave equation; (b) x- and (e) z-components synthesized by pseudo-pure-mode qP-wave equation; (c) pseudo-pure-mode scalar qP-wave fields; (f) separated scalar qP-wave fields.

1.3 BP 2007 TTI model

Next we test the approach of simulating propagation of the separated qP-wave mode in a complex TTI model. Figure 7 shows parameters for part of the BP 2D TTI model. The space grid size is 12.5 m and the time step is 1 ms for high-order finite-difference operators. Here the vertical velocities for the qSV-wave are set as half of the qP-wave velocities. Figure 8 displays snapshots of wavefield components at the time of 1.4s synthesized by using original elastic wave equation and pseudo-pure-mode qP-wave equation. The two pictures at the bottom represent the scalar pseudo-pure-mode qP-wave and the separated qP-wave fileds, respectively. The correction appears to remove residual qSV-waves and accurately separate qP-wave data including the converted qS-qP waves from the pseudo-pure-mode wavefields in this complex model.

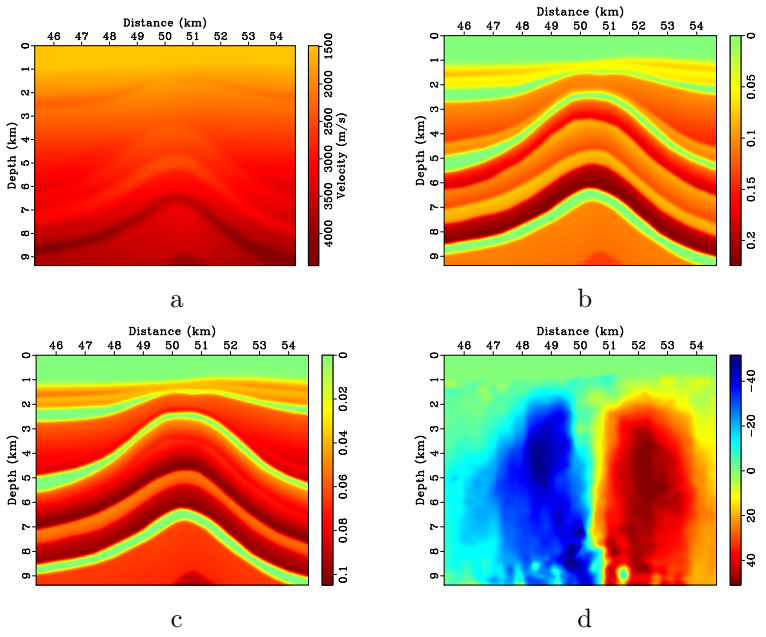

Figure 7: Partial region of the 2D BP TTI model: (a) vertical qP-wave velocity, Thomsen coefficients (b) ϵ and (c) δ, and (d) the tilt angle θ.

1.4 Homogeneous 3D ORT model

Figure 9 shows an example of simulating propagation of separated qP-wave fields in a 3D homogeneous vertical ORT model, in which $v_{p0} = 3000m/s$, $v_{s0} = 1500m/s$, $\delta_1 = -0.1$, $\delta_2 = -0.0422$, $\delta_3 = 0.125$, $\epsilon_1 = 0.2$, $\epsilon_2 = 0.067$, $\gamma_1 = 0.1$, and $\gamma_2 = 0.047$. The first three pictures display wavefield snapshots at 0.5s synthesized by using pseudo-pure-mode qP-wave equation, according to equation B-3. As shown in Figure 9d, qP-waves again appear to dominate the wavefields in energy when we sum the three wavefield components of the pseudo-pure-mode qP-wave fields. As for TI media, we obtain completely separated qP-wave fields from the pseudo-pure-mode wavefields once the correction of projection deviation is finished (Figure 9e). By the way, in

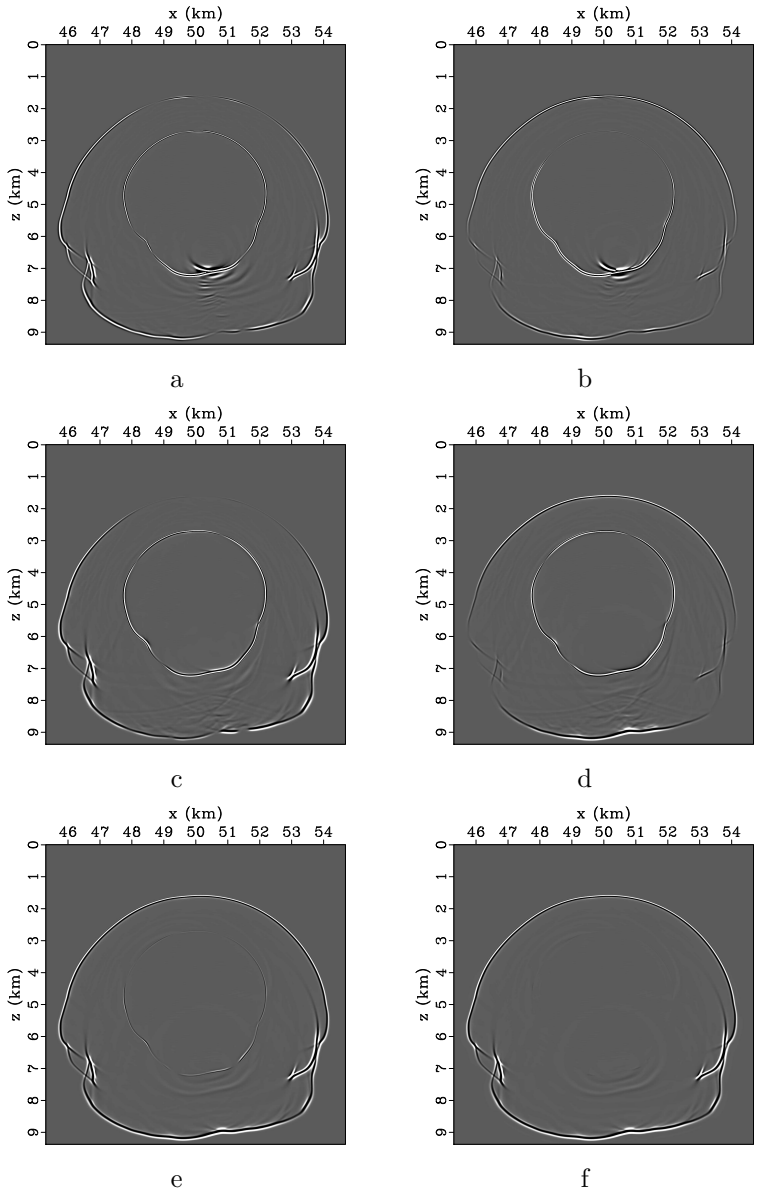

Figure 8: Synthesized elastic wavefields on BP 2007 TTI model using original elastic wave equation and pseudo-pure-mode qP-wave equation respectively: (a) x- and (b) z-components synthesized by original elastic wave equation; (c) x- and (d) z-components synthesized by pseudo-pure-mode qP-wave equation; (e) pseudo-pure-mode scalar qP-wave fields; (f) separated scalar qP-wave fields.

all above examples, we find that the filtering to remove qSV-waves does not require the numerical dispersion of the qS-waves to be limited. So there is no additional requirement of the grid size for qS-wave propagation. The effects of grid dispersion for the separation of low velocity qS-waves will be further investigated in the second article of this series.

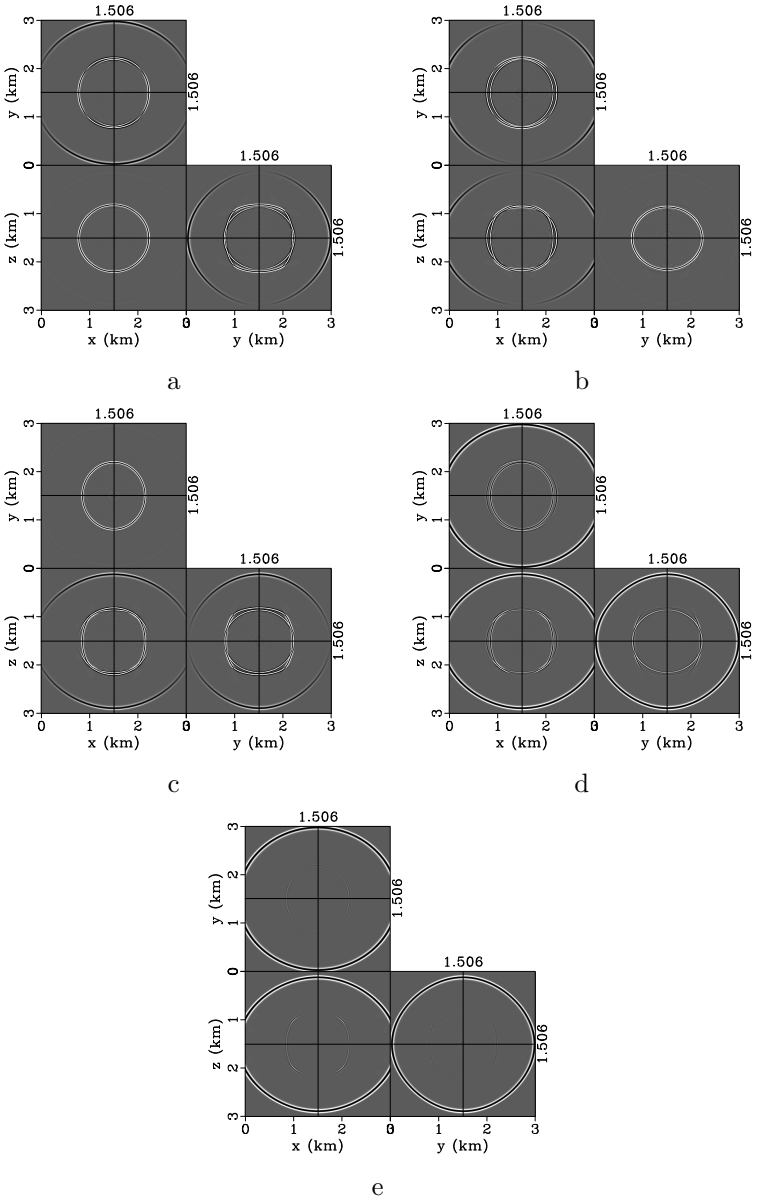

Figure 9: Synthesized wavefield snapshots in a 3D homogeneous vertical ORT medium: (a) x-, (b) y- and (c) z-component of the pseudo-pure-mode qP-wave fields, (d) pseudo-pure-mode scalar qP-wave fields, (e) separated scalar qP-wave fields.

2. Reverse-time migration of Hess VTI model

Our final example shows application of the pseudo-pure-mode qP-wave equation (i.e., equation 22 in its 2D form) to RTM of conventional seismic data representing mainly qP-wave energy using the synthetic data of SEG/Hess VTI model (Figure 10). In the original data set, there is no vertical velocity model for qSV-wave, namely v_{s0}. For simplicity, we first get this parameter by setting $\frac{v_{s0}}{v_{p0}} = 0.5$ anywhere. Figures 11a and 11b display the two components of the synthesized pseudo-pure-mode qP-wave fields, in which the source is located at the center of the windowed region of the original models. We observe that the summed wavefields (i.e., pseudo-pure-mode scalar qP-wave fields) contain quite weak residual qSV-wave energy (Figure 11c). For seismic imaging of qP-wave data, we try the finite nonzero v_{s0} scheme (Fletcher et al., 2009) to suppress qSV-wave artifacts and enhance computation stability. Thanks to superposition of multi-shot migrated data, we obtain a good RTM result (Figure 12) using the common-shot gathers provided at http://software.seg.org, although spatial filtering has not been used to remove the residual qSV-wave energy. This example shows that the proposed pseudo-pure-mode qP-wave equation could be directly used for reverse-time migration of conventional single-component seismic data.

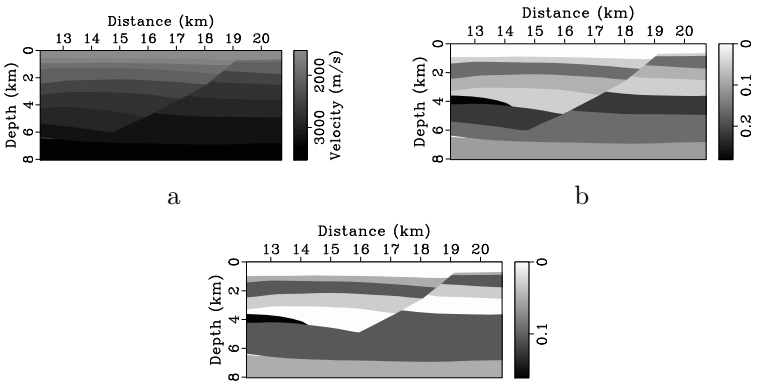

Figure 10: Part of SEG/Hess VTI model with parameters of (a) vertical qP-wave velocity, Thomsen coefficients (b) ϵ and (c) δ.

DISCUSSION

For the general anisotropic media, qP- and qS-wave modes are intrinsically coupled. The elastic wave equation must be solved at once to get correct kinematics and amplitudes for all modes. The scalar wavefields, however, are widely used with the help of wave mode separation or by using approximate equations derived from the elastic wave equation for many applications such as seismic imaging. As demonstrated in the theoretical parts, the pseudo-pure-mode wave equation is derived from the elastic wave equation through a similarity transformation to the Christoffel equation in the

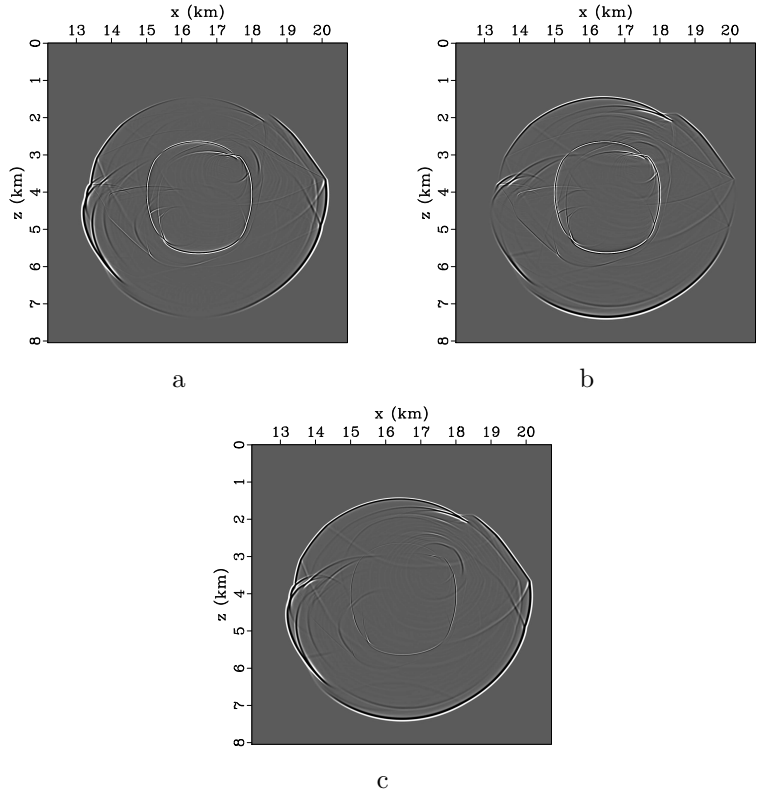

Figure 11: Synthesized wavefields using the pseudo-pure-mode qP-wave equation in SEG/Hess VTI model: The three snapshots are synthesized by fixing the ratio of v_{s0} to v_{p0} as 0.5. The pseudo-pure-mode qP-wave fields (c) are the sum of the (a) x- and (b) z-components of the pseudo-pure-mode wavefields.

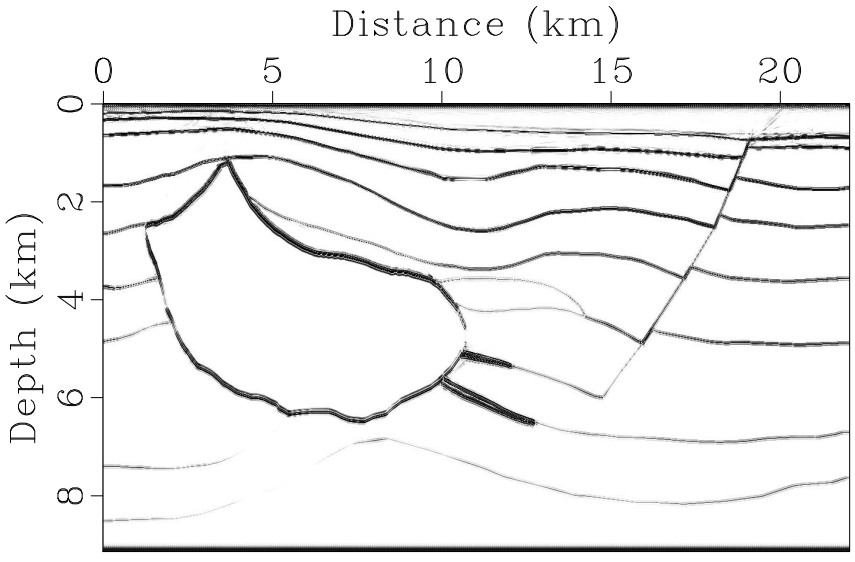

Figure 12: RTM of Hess VTI model using the pseudo-pure-mode qP-wave equation with nonzero finite v_{s0}.

wavenumber domain. The components of the transformed wavefield essentially represent the spatial derivatives of the displacement wavefield components. This transformation preserves the kinematics of wave propagation but inevitablely changes the phases and amplitudes for qP- and qS-waves as the elastic wave mode separation procedure using divergence-like and curl-like operations (Dellinger and Etgen, 1990; Yan and Sava, 2009; Zhang and McMechan, 2010). The filtering step to correct the projection deviation is indispensable for complete removing the residual qS-waves from the extrapolated pseudo-pure-mode qP-wave fields. This procedure does not change the phases and amplitudes of the scalar qP-waves because the deviation operator is computed using the normalized wave and polarization vectors.

In fact, it is not even clear what the correct amplitudes should be for "scalar anisotropy". Like the anisotropic pseudo-analytic methods (Etgen and Brandsberg-Dahl, 2009; Fomel et al., 2013; Zhan et al., 2012; Song and Alkhalifah, 2013), the pseudo-pure-mode wave equation may distort the reflection, transmission and conversion coefficients of the elastic wavefields when there are high-frequency perturbations in the velocity model. Therefore, the converted qP-waves remaining in the separated qP-wave fileds only have reliable kinematics. What happens to the qP-wave's amplitudes and how to make use of the converted qP-waves (for seismic imaging) on the base of the pseudo-pure-mode qP-wave equation need further investigation in our future research.

CONCLUSIONS

We have proposed an alternative approach to simulate propagation of separated wave modes in general anisotropic media. The key idea is splitting the one-step wave mode separation into two cascaded steps based on the following observations: First, the Christoffel equation derived from the original elastic wave equation accurately represents the kinematics of all wave modes; Second, various coupled second-order wave equations can be derived from the Christoffel equation through similarity transformations. Third, wave mode separation can be achieved by projecting the original elastic wavefields onto the given mode's polarization directions, which are usually calculated based on the local material parameters using the Christoffel equation. Accordingly, we have derived the pseudo-pure-mode qP-wave equation by applying a similarity transformation aiming to project the elastic wavefield onto the wave vector, which is the isotropic references of qP-wave polarization for an anisotropic medium. The derived pseudo-pure-mode equations not only describe propagation of all wave modes but also implicitly achieve partial mode separation once the wavefield components are summed. As shown in the examples, the scalar pseudo-pure-mode qP-wave fields are dominated by qP-waves while the residual qS-waves are weaker in energy, because the projection deviations of qP-waves are generally far less than those of the qSV-waves. Synthetic example of Hess VTI model demonstrates successful application of the pseudo-pure-mode qP-wave equation to RTM for conventional seismic exploration. To completely remove the residual qS-waves, a filtering step has been proposed to

correct the projection deviations resulting from the difference between polarization direction and its isotropic reference. In homogeneous media, it can be efficiently implemented by applying wavenumber domain filtering to each wavefield component. In heterogeneous media, nonstationary spatial filtering using pseudo-derivative operators are applied to finish the second step for wave mode separation. In a word, pseudo-pure-mode wave equations plus corrections of projection deviations provide us an efficient and flexible tool to simulate propagation of separated wave modes in anisotropic media.

In spite of the amplitude properties, this approach has some advantages over the classical solution combining elastic wavefield extrapolation and wave mode separation: First, the pseudo-pure-mode wave equations could be directly used for migration of seismic data recorded with single-component geophones without computationally expensive wave mode separation (as shown in the last example). Second, because partial wave mode separation is automatically achieved during wavefield extrapolation and the correction step to remove the residual qS-waves is optional depending on the strength of anisotropy, our approach provides better flexibilty for seismic modeling, migration and parameter inversion in practice; Third, computational cost is reduced at least one third for the 2D cases if the finite difference algorithms are used thanks to the simpler structure of pseudo-pure-mode wave equations (i.e., having no mixed derivative terms for VTI and vertically orthorhombic media). For the 3D TI media, computational cost is further reduced about one third because two instead of three equations are used to simulate wave propagation.

Unlike the pseudo-acoustic wave equations, pseudo-pure-mode wave equations have no approximation in kinematics and allow for $\epsilon < \delta$ provided that the stiffness tensor is positive-definite. Moreover, they provide a possibility to extract artifact-free separated wave mode during wavefield extrapolation. Although we focus on propagation of separated qP-waves using the pseudo-pure-mode qP-wave equation, our approach also works for qS-waves in TI media. This will be demonstrated in the second paper of this series.

ACKNOWLEDGMENTS

The research leading to this paper was supported by the National Natural Science Foundation of China (No.41074083) and the Fundamental Research Funds for the Central Universities (No.1350219123). We would like to thank Sergey Fomel, Paul Fowler, Yu Zhang, Tengfei Wang and Chenlong Wang for helpful discussions in the later period of this study. Constructive comments by Joe Dellinger, Faqi Liu, Mirko van der Baan, Reynam Pestana, and an anonymous reviewer are much appreciated. We thank SEG, HESS Corporation and BP for making the 2D VTI and TTI synthetic data sets available, and the authors of *Madagascar* for providing this software platform for reproducible computational experiments.

APPENDIX A

PSEUDO-PURE-MODE QP-WAVE EQUATION FOR VERTICAL TI AND ORTHORHOMBIC MEDIA

For vertical TI and orthorhombic media, the stiffness tensors have the same null components and can be represented in a two-index notation (Musgrave, 1970) often called the Voigt notation as

$$\mathbf{C} = \begin{pmatrix} C_{11} & C_{12} & C_{13} & 0 & 0 & 0 \\ C_{12} & C_{22} & C_{23} & 0 & 0 & 0 \\ C_{13} & C_{23} & C_{33} & 0 & 0 & 0 \\ 0 & 0 & 0 & C_{44} & 0 & 0 \\ 0 & 0 & 0 & 0 & C_{55} & 0 \\ 0 & 0 & 0 & 0 & 0 & C_{66} \end{pmatrix}. \tag{A-1}$$

For vertical orthorhombic tensor, the nine coefficients are indepedent, but the VTI tensor has only five independent coefficients with $C_{12} = C_{11} - 2C_{66}$, $C_{22} = C_{11}$, $C_{23} = C_{13}$ and $C_{55} = C_{44}$. The stability condition requires these parameters to satisfy the corresponding constraints (Helbig, 1994; Tsvankin, 2001). According to equations 3 and 4, the full elastic wave equation without the source terms is expressed as:

$$\begin{aligned} \rho\frac{\partial^2 u_x}{\partial t^2} &= C_{11}\frac{\partial^2 u_x}{\partial x^2} + C_{66}\frac{\partial^2 u_x}{\partial y^2} + C_{55}\frac{\partial^2 u_x}{\partial z^2} + (C_{12}+C_{66})\frac{\partial^2 u_y}{\partial x \partial y} + (C_{13}+C_{55})\frac{\partial^2 u_z}{\partial x \partial z}, \\ \rho\frac{\partial^2 u_y}{\partial t^2} &= C_{66}\frac{\partial^2 u_y}{\partial x^2} + C_{22}\frac{\partial^2 u_y}{\partial y^2} + C_{44}\frac{\partial^2 u_y}{\partial z^2} + (C_{12}+C_{66})\frac{\partial^2 u_x}{\partial x \partial y} + (C_{23}+C_{44})\frac{\partial^2 u_z}{\partial y \partial z}, \\ \rho\frac{\partial^2 u_z}{\partial t^2} &= C_{55}\frac{\partial^2 u_z}{\partial x^2} + C_{44}\frac{\partial^2 u_z}{\partial y^2} + C_{33}\frac{\partial^2 u_z}{\partial z^2} + (C_{13}+C_{55})\frac{\partial^2 u_x}{\partial x \partial z} + (C_{23}+C_{44})\frac{\partial^2 u_y}{\partial y \partial z}. \end{aligned} \tag{A-2}$$

Thus the corresponding Christoffel matrix in wavenumber domain satisfies

$$\widetilde{\mathbf{\Gamma}} = \begin{pmatrix} C_{11}{k_x}^2 + C_{66}{k_y}^2 + C_{55}{k_z}^2 & (C_{12}+C_{66})k_x k_y & (C_{13}+C_{55})k_x k_z \\ (C_{12}+C_{66})k_x k_y & C_{66}{k_x}^2 + C_{22}{k_y}^2 + C_{44}{k_z}^2 & (C_{23}+C_{44})k_y k_z \\ (C_{13}+C_{55})k_x k_z & (C_{23}+C_{44})k_y k_z & C_{55}{k_x}^2 + C_{44}{k_y}^2 + C_{33}{k_z}^2 \end{pmatrix}. \tag{A-3}$$

According to equation 10, the Christoffel matrix after the similarity transformation is given as,

$$\widetilde{\overline{\mathbf{\Gamma}}} = \begin{pmatrix} C_{11}{k_x}^2 + C_{66}{k_y}^2 + C_{55}{k_z}^2 & (C_{12}+C_{66}){k_x}^2 & (C_{13}+C_{55}){k_x}^2 \\ (C_{12}+C_{66}){k_y}^2 & C_{66}{k_x}^2 + C_{22}{k_y}^2 + C_{44}{k_z}^2 & (C_{23}+C_{44}){k_y}^2 \\ (C_{13}+C_{55}){k_z}^2 & (C_{23}+C_{44}){k_z}^2 & C_{55}{k_x}^2 + C_{44}{k_y}^2 + C_{33}{k_z}^2 \end{pmatrix}. \tag{A-4}$$

Finally, we obtain the pseudo-pure-mode qP-wave equation (i.e., equation 18) by inserting equation A-4 into equation 12 and applying an inverse Fourier transform.

APPENDIX B

PSEUDO-PURE-MODE QP-WAVE EQUATION IN ORTHORHOMBIC MEDIA

One of the most common reasons for orthorhombic anisotropy in sedimentary basins is a combination of parallel vertical fractures and vertically transverse isotropy in the background medium (Wild and Crampin, 1991; Schoenberg and Helbig, 1997). Vertically orthorhombic models have three mutually orthogonal planes of mirror symmetry that coincide with the coordinate planes $[x_1, x_2]$, $[x_1, x_3]$ and $[x_2, x_3]$. Here we assume x_1 axis is the x-axis (and used as the symmetry axis), x_2 the y-axis, and x_3 the z-axis. Using the Thomsen-style notation for orthorhombic media (Tsvankin, 1997):

$$
\begin{aligned}
v_{p0} &= \sqrt{\frac{C_{33}}{\rho}}, \\
v_{s0} &= \sqrt{\frac{C_{55}}{\rho}}, \\
\epsilon_1 &= \frac{C_{22} - C_{33}}{2C_{33}}, \\
\delta_1 &= \frac{(C_{23} + C_{44})^2 - (C_{33} - C_{44})^2}{2C_{33}(C_{33} - C_{44})}, \\
\gamma_1 &= \frac{C_{66} - C_{55}}{2C_{55}}, \\
\epsilon_2 &= \frac{C_{11} - C_{33}}{2C_{33}}, \\
\delta_2 &= \frac{(C_{13} + C_{55})^2 - (C_{33} - C_{55})^2}{2C_{33}(C_{33} - C_{55})}, \\
\gamma_2 &= \frac{C_{66} - C_{44}}{2C_{44}}, \\
\delta_3 &= \frac{(C_{12} + C_{66})^2 - (C_{11} - C_{66})^2}{2C_{11}(C_{11} - C_{66})},
\end{aligned}
\tag{B-1}
$$

and

$$
\begin{aligned}
v_{px1} &= v_{p0}\sqrt{1 + 2\epsilon_1}, \\
v_{px2} &= v_{p0}\sqrt{1 + 2\epsilon_2}, \\
v_{sx1} &= v_{s0}\sqrt{1 + 2\gamma_1}, \\
v_{sx2} &= v_{s0}\sqrt{1 + 2\gamma_2}, \\
v_{pn1} &= v_{p0}\sqrt{1 + 2\delta_1}, \\
v_{pn2} &= v_{p0}\sqrt{1 + 2\delta_2}, \\
v_{pn3} &= v_{p0}\sqrt{1 + 2\delta_3},
\end{aligned}
\tag{B-2}
$$

the pseudo-pure-mode qP-wave equation (equation 18) is rewritten as,

$$\begin{aligned}
\frac{\partial^2 \overline{u}_x}{\partial t^2} &= v_{px2}^2 \frac{\partial^2 \overline{u}_x}{\partial x^2} + v_{sx1}^2 \frac{\partial^2 \overline{u}_x}{\partial y^2} + v_{s0}^2 \frac{\partial^2 \overline{u}_x}{\partial z^2} + \sqrt{(v_{px2}^2 - v_{sx1}^2)[(1+2\epsilon_2)v_{pn3}^2 - v_{sx1}^2]} \frac{\partial^2 \overline{u}_y}{\partial x^2} \\
&\quad + \sqrt{(v_{p0}^2 - v_{s0}^2)(v_{pn2}^2 - v_{s0}^2)} \frac{\partial^2 \overline{u}_z}{\partial x^2}, \\
\frac{\partial^2 \overline{u}_y}{\partial t^2} &= v_{sx1}^2 \frac{\partial^2 \overline{u}_y}{\partial x^2} + v_{px1}^2 \frac{\partial^2 \overline{u}_y}{\partial y^2} + v_{s12}^2 \frac{\partial^2 \overline{u}_y}{\partial z^2} + \sqrt{(v_{px2}^2 - v_{sx1}^2)[(1+2\epsilon_2)v_{pn3}^2 - v_{sx1}^2]} \frac{\partial^2 \overline{u}_x}{\partial y^2} \\
&\quad + \sqrt{(v_{p0}^2 - v_{s12}^2)(v_{pn1}^2 - v_{s12}^2)} \frac{\partial^2 \overline{u}_z}{\partial y^2}, \\
\frac{\partial^2 \overline{u}_z}{\partial t^2} &= v_{s0}^2 \frac{\partial^2 \overline{u}_z}{\partial x^2} + v_{s12}^2 \frac{\partial^2 \overline{u}_z}{\partial y^2} + v_{p0}^2 \frac{\partial^2 \overline{u}_z}{\partial z^2} + \sqrt{(v_{p0}^2 - v_{s0}^2)(v_{pn2}^2 - v_{s0}^2)} \frac{\partial^2 \overline{u}_x}{\partial z^2} \\
&\quad + \sqrt{(v_{p0}^2 - v_{s12}^2)(v_{pn1}^2 - v_{s12}^2)} \frac{\partial^2 \overline{u}_y}{\partial z^2},
\end{aligned} \tag{B-3}$$

where v_{p0} represents the vertical velocity of qP-wave, v_{s0} represents the vertical velocity of qS-waves polarized in the x_1 direction, ϵ_1, δ_1 and γ_1 represent the VTI parameters ϵ, δ and γ in the $[y, z]$ plane, ϵ_2, δ_2 and γ_2 represent the VTI parameters ϵ, δ and γ in the $[x, z]$ plane, δ_3 represents the VTI parameter δ in the $[x, y]$ plane. v_{px1} and v_{px2} are the horizontal velocities of qP-wave in the symmetry planes normal to the x- and y-axis, respectively. v_{pn1}, v_{pn2} and v_{pn3} are the interval NMO velocities in the three symmetry planes, and $v_{s12} = v_{s0}\sqrt{\frac{1+2\gamma_1}{1+2\gamma_2}}$.

Setting $v_{s0} = 0$, we further obtain the pseudo-acoustic coupled system in a vertically orthorhombic media,

$$\begin{aligned}
\frac{\partial^2 \overline{u}_x}{\partial t^2} &= v_{px2}^2 \frac{\partial^2 \overline{u}_x}{\partial x^2} + (1+2\epsilon_2)\sqrt{1+2\delta_3}\, v_{p0}^2 \frac{\partial^2 \overline{u}_y}{\partial x^2} + \sqrt{1+2\delta_2}\, v_{p0}^2 \frac{\partial^2 \overline{u}_z}{\partial x^2}, \\
\frac{\partial^2 \overline{u}_y}{\partial t^2} &= (1+2\epsilon_2)\sqrt{1+2\delta_3}\, v_{p0}^2 \frac{\partial^2 \overline{u}_x}{\partial y^2} + (1+2\epsilon_1) v_{p0}^2 \frac{\partial^2 \overline{u}_y}{\partial y^2} + \sqrt{1+2\delta_1}\, v_{p0}^2 \frac{\partial^2 \overline{u}_z}{\partial y^2}, \\
\frac{\partial^2 \overline{u}_z}{\partial t^2} &= \sqrt{1+2\delta_2}\, v_{p0}^2 \frac{\partial^2 \overline{u}_x}{\partial z^2} + \sqrt{1+2\delta_1}\, v_{p0}^2 \frac{\partial^2 \overline{u}_y}{\partial z^2} + v_{p0}^2 \frac{\partial^2 \overline{u}_z}{\partial z^2}.
\end{aligned} \tag{B-4}$$

Note that this equation does not contain any of the parameters γ_1 and γ_2 that describe the shear-wave velocities in the directions of the x- and y-axis, respectively. Evidently, kinematic signatures of qP-waves in pseudo-acoustic orthorhombic media depend on just five anisotropic coefficients (ϵ_1, ϵ_2, δ_1, δ_2 and δ_3) and the vertical velocity v_{p0}.

In the presence of dipping fracture, we need to extend the vertically orthorhombic symmetry to a more complex form, i.e. orthorhombic media with tilted symmetry planes. Similar to TTI media, we locally rotate the coordinate system to make use of the simple form of the pseudo-pure-mode wave equations in vertically orthorhombic media. Since the physical properties are not symmetric in the local $[x_1; x_2]$ plane, we need three angles to describe the rotation (Zhang and Zhang, 2011). Two angles, θ and φ, are used to define the vertical axis at each spatial point as we did for the

symmetry axis in TTI model. The third angle α is introduced to rotate the stiffness tensor on the local plane and to represent the orientation of the fracture system in a VTI background or the orientation of the first fracture system of two orthogonal ones in an isotropic background.

The second-order differential operators in the rotated coordinate system are expressed in the same forms as in equation 28, but the rotation matrix is now given by,

$$\mathbf{R} = \begin{pmatrix} \cos\varphi & -\sin\varphi & 0 \\ \sin\varphi & \cos\varphi & 0 \\ 0 & 0 & 1 \end{pmatrix} \begin{pmatrix} \cos\theta & 0 & \sin\theta \\ 0 & 1 & 0 \\ -\sin\theta & 0 & \cos\theta \end{pmatrix} \begin{pmatrix} \cos\alpha & -\sin\alpha & 0 \\ \sin\alpha & \cos\alpha & 0 \\ 0 & 0 & 1 \end{pmatrix}, \tag{B-5}$$

where

$$\begin{aligned} r_{11} &= \cos\theta\cos\varphi\cos\alpha - \sin\varphi\sin\alpha, \\ r_{12} &= -\cos\theta\cos\varphi\sin\alpha - \sin\varphi\cos\alpha, \\ r_{13} &= \sin\theta\cos\varphi, \\ r_{21} &= \cos\theta\sin\varphi\cos\alpha + \cos\varphi\sin\alpha, \\ r_{22} &= -\cos\theta\sin\varphi\sin\alpha + \cos\varphi\cos\alpha, \\ r_{23} &= \sin\theta\sin\varphi, \\ r_{31} &= -\sin\theta\cos\alpha, \\ r_{32} &= \sin\theta\sin\alpha, \\ r_{33} &= \cos\theta. \end{aligned} \tag{B-6}$$

Substituting the second-order differential operators into the rotated coordinate system for those in the pseudo-pure-mode qP-wave equation of vertically orthorhombic media yields the pseudo-pure-mode qP-wave equation of tilted orthorhombic media in the global Cartesian coordinates.

APPENDIX C

DEVIATION BETWEEN PHASE NORMAL AND POLARIZATION DIRECTION OF QP-WAVES IN VTI MEDIA

For VTI media, Dellinger (1991) presents an expression of the deviation angle ζ between the phase normal (with phase angle ψ) and the polarization direction of qP-waves, namely

$$\sin^2(\zeta) = \frac{1}{2} + \frac{[(2s-1)t_1 - t_2]\sqrt{t_1^2 - t_2\chi}}{2(t_2\chi - {t_1}^2)}, \tag{C-1}$$

where

$$\begin{aligned} s &= \sin^2(\psi), \\ t_1 &= s(C_{33} + C_{11} - 2C_{44}) - C_{33} + C_{44} \\ &= s\rho[v_{p0}^2 + (1+2\epsilon)v_{p0}^2 - 2v_{s0}^2] - \rho v_{p0}^2 + \rho v_{s0}^2, \\ t_2 &= 4s(s-1)\chi, \\ \chi &= C_{13} + C_{44} \\ &= \rho\sqrt{(v_{p0}^2 - v_{s0}^2)(v_{pn}^2 - v_{s0}^2)}. \end{aligned} \tag{C-2}$$

Equation C-1 indicates that the deviation angle has a complicated nonlinear relation with anisotropic parameters and the phase angle. The relationship is rather lengthy and does not easily reveal the features caused by anisotropy. Hence we use an alternative expression under a weak anisotropy assumption (Rommel, 1994; Tsvankin, 2001),

$$\zeta = \frac{[\delta + 2(\epsilon - \delta)\sin^2\psi]\sin 2\psi}{2(1 - \frac{v_{s0}^2}{v_{p0}^2})} \tag{C-3}$$

It appears that the deviation angle is mainly affected by the difference between ϵ and δ, the magnitude of δ (when $\epsilon - \delta$ stays the same) and the ratio of vertical velocities of qP- and qS-wave, as well as the phase angle.

REFERENCES

Alkhalifah, T., 2000, An acoustic wave equation for anisotropic media: Geophysics, **65**, 1239–1250.

———, 2003, An acoustic wave equation for orthorhombic anisotropy: Geophysics, **68**, 1169–1172.

Auld, B., 1973, Acoustic fields and waves in solids: John Wiley & Sons, New York.

Bube, K. P., T. Nemeth, J. P. Stefani, R. Ergas, W. Liu, K. T. Nihei, and L. Zhang, 2012, On the instability in second-order systems for acoustic VTI and TTI media: Geophysics, **77**, T171–T186.

Carcione, J. M., 2001, Wave fields in real media: Wave propagation in anisotropic, anelastic and porous media: Pergamon Press.

Cheng, J. B., and S. Fomel, 2013, Fast algorithms for elastic wave mode separation and vector decomposition using low-rank approximation for anisotropic media: 83rd Annual International Meeting, SEG, Expanded Abstracts, 991–997.

Cheng, J. B., and W. Kang, 2012, Propagating pure wave modes in general anisotropic media, Part I: P-wave propagator: 82nd Annual International Meeting, SEG, Expanded Abstracts, doi: 10.1190/segam2012–0616.1.

Chu, C., B. Macy, and P. Anno, 2011, Approximation of pure acoustic seismic wave propagation in TTI media: Geophysics, **76**, WB98–WB107.

Crampin, S., 1984, Effective anisotropic elastic constants for wave propagation through cracked solids: Geophysical Journal of the Royal Astronomical Society, **76**, 135–145.

Dellinger, J., 1991, Anisotropic seismic wave propagation: PhD thesis, Stanford University.

Dellinger, J., and J. Etgen, 1990, Wavefield separation in two-dimensional anisotropic media: Geophysics, **55**, 914–919.

Du, X., R. P. Fletcher, and P. J. Fowler, 2010, Pure p-wave propagators versus pseudo-acoustic propagators for RTM in VTI media: 72nd Annual International Meeting, EAGE, Expanded Abstracts, 382–386.

Duveneck, E., and P. M. Bakker, 2011, Stable P-wave modeling for reverse-time migration in tilted TI media: Geophysics, **76**, S65–S75.

Etgen, J., and S. Brandsberg-Dahl, 2009, The pseudo-analytical method: Application of pseudo-Laplacians to acoustic and acoustic anisotropic wave propagation: 79th Annual International Meeting, SEG, Expanded Abstracts, 2552–2556.

Fletcher, R. P., X. Du, and P. J. Fowler, 2009, Reverse time migration in tilted transversely isotropic (TTI) media: Geophysics, **74**, WCA179–WCA187.

Fomel, S., L. Ying, and X. Song, 2013, Seismic wave extrapolation using lowrank symbol approximation: Geophysical Prospecting, **61**, 526–536.

Fowler, P., and R. King, 2011, Modeling and reverse time migration of orthorhombic pseudo-acoustic P-waves: 81st Annual International Meeting, SEG, Expanded Abstracts, 190–195.

Fowler, P. J., X. Du, and R. P. Fletcher, 2010, Coupled equations for reverse time migration in transversely isotropic media: Geophysics, **75**, S11–S22.

Grechka, V., L. Zhang, and J. W. R. III, 2004, Shear waves in acoustic anisotropic

media: Geophysics, **69**, 576–582.
Helbig, K., 1994, Foundation of anisotropy for exploration seismics: Pergamon Press.
Hestholm, S., 2007, Acoustic VTI modeling using high-order finite-differences: 77th Annual International Meeting, SEG, Expanded Abstracts, 139–143.
Jin, S., F. Jiang, and Y. Ren, 2011, Comparison of isotropic, VTI and TTI reverse time migration: an experiment on BP anisotropic benchmark dataset: 81st Annual International Meeting, SEG, Expanded Abstracts, 3198–3203.
Kang, W., and J. B. Cheng, 2011, New coupled equations of P- and SV-wave for RTM in TI media: 73rd Annual International Meeting, EAGE, Expanded Abstracts, P267.
———, 2012, Propagating pure wave modes in 3D general anisotropic media, Part II: SV and SH wave: 82nd Annual International Meeting, SEG, Expanded Abstracts, doi: 10.1190/segam2012–1234.1.
Klie, H., and W. Toro, 2001, A new acoustic wave equation for modeling in anisotropic media: 71st Annual International Meeting, SEG, Expanded Abstracts, 1171–1174.
Liu, F., S. Morton, S. Jiang, L. Ni, and J. Leveille, 2009, Decoupled wave equations for P and SV waves in an acoustic VTI media: 79th Annual International Meeting, SEG, Expanded Abstracts, 2844–2848.
Macesanu, 2011, The pseudo-acoustic approximation to wave propagation in TTI media: 81st Annual International Meeting, SEG, Expanded Abstracts, 174–178.
Musgrave, M. J. P., 1970, Crystal acoustics: Holden Day.
Pestana, R., and P. L. Stoffa, 2010, Time evolution of the wave equation using rapid expansion method: Geophysics, **75**, T121–T131.
Pestana, R., B. Ursin, and P. L. Stoffa, 2011, Separate P- and SV-wave equations for VTI media: SEG Technical Program Expanded Abstracts, 163–167.
Psencik, I., and D. Gajewski, 1998, Polarization, phase velocity, and NMO velocity of qP-waves in arbitrary weak anisotropic media: Geophysics, **63**, 1754–1766.
Rommel, B. E., 1994, Approximate polarization of plane waves in a medium having weak transverse isotropy: Geophysics, **59**, 1605–1612.
Schoenberg, M., and K. Helbig, 1997, Orthorhombic media: Modeling elastic wave behavior in a vertically fractured earth: Geophysics, **62**, 1954–1974.
Song, X., and T. Alkhalifah, 2013, Modeling of pseudoacoustic p-waves in orthorhombic media with a low-rank approximation: Geophysics, **78**, C33–C40.
Song, X., and S. Fomel, 2011, Fourier finite-difference wave propagation: Geophysics, **76**, T123–T129.
Thomsen, L., 1986, Weak elastic anisotropy: Geophysics, **51**, 1954–1996.
Tsvankin, I., 1997, Anisotropic parameters and P-wave velocity for orthorhombic media: Geophysics, **62**, 1292–1309.
———, 2001, Seismic signatures and analysis of reflection data in anisotropioc media: Elsevier Science Ltd.
Tsvankin, I., and E. Chesnokov, 1990, Synthesis of body-wave seismograms from point source in anisotropic media: Journal of Geophysics Research, **95**, 11317–11331.
Wild, P., and S. Crampin, 1991, The range of effects of azimuthal isotropy and EDA anisotropy in sedimentary basins: Geophysical Journal of International, **107**, 513–529.

Winterstein, D., 1990, Velocity anisotropy terminology for geophysicists: Geophysics, **55**, 1070–1088.

Yan, J., and P. Sava, 2009, Elastic wave-mode separation for VTI media: Geophysics, **74**, WB19–WB32.

———, 2011, Improving the efficiency of elastic wave-mode separation for heterogenous tilted transver isotropic media: Geophysics, **76**, T65–T78.

———, 2012, Elastic wave mode separation for tilted transversely isotropic media: Geophysical Prospecting, **60**, 29–48.

Yilmaz, O., 2001, Seismic data analysis: Processing, inversion, and interpretation of seismic data (second edition): Society of Exploration Geophysics.

Zhan, G., R. C. Pestana, and P. L. Stoffa, 2012, Decoupled equations for reverse time migration in tilted transversely isotropic media: Geophysics, **77**, T37–T45.

Zhang, H., G. Zhang, and Y. Zhang, 2009, Removing S-wave noise in TTI reverse time migration: 79th Annual International Meeting, SEG, Expanded Abstracts, 2849–2853.

Zhang, H., and Y. Zhang, 2011, Reverse time migration in vertical and tilted orthorhombic media: 81st Annual International Meeting, SEG, Expanded Abstracts, 185–189.

Zhang, L., J. W. R. III, and G. M. Hoversten, 2003, An acoustic wave equation for modeling in tilted TI media: 73rd Annual International Meeting, SEG, Expanded Abstracts, 153–156.

Zhang, Q., and G. A. McMechan, 2010, 2D and 3D elastic wavefield vector decomposition in the wavenumber domain for VTI media: Geophysics, **75**, D13–D26.

Zhang, Y., and G. Zhang, 2009, One-step extrapolation method for reverse time migration: Geophysics, **74**, A29–A33.

Zhang, Y., H. Zhang, and G. Zhang, 2011, A stable TTI reverse time migration and its implementation: Geophysics, **76**, WA3–WA11.

Zhou, H., G. Zhang, and R. Bloor, 2006a, An anisotropic acoustic wave equation for modeling and migration in 2D TTI media: 76th Annual International Meeting, SEG, Expanded Abstracts, 194–198.

———, 2006b, An anisotropic acoustic wave equation for VTI media: 68th Annual International Meeting, EAGE, Expanded Abstracts, 1171–1174.